LR-GLM: High-Dimensional Bayesian Inference Using Low-Rank Data Approximations

Brian L. Trippe 1 Jonathan H. Huggins 2 Raj Agrawal 1 Tamara Broderick 1

Abstract

Due to the ease of modern data collection, applied statisticians often have access to a large set of covariates that they wish to relate to some observed outcome. Generalized linear models (GLMs) offer a particularly interpretable framework for such an analysis. In these high-dimensional problems, the number of covariates is often large relative to the number of observations, so we face non-trivial inferential uncertainty; a Bayesian approach allows coherent quantification of this uncertainty. Unfortunately, existing methods for Bayesian inference in GLMs require running times roughly cubic in parameter dimension, and so are limited to settings with at most tens of thousand parameters. We propose to reduce time and memory costs with a low-rank approximation of the data in an approach we call LR-GLM. When used with the Laplace approximation or Markov chain Monte Carlo, LR-GLM provides a full Bayesian posterior approximation and admits running times reduced by a full factor of the parameter dimension. We rigorously establish the quality of our approximation and show how the choice of rank allows a tunable computational-statistical trade-off. Experiments support our theory and demonstrate the efficacy of LR-GLM on real large-scale datasets.

1. Introduction

Scientists, engineers, and social scientists are often interested in characterizing the relationship between an outcome and a set of covariates, rather than purely optimizing predictive accuracy. For example, a biologist may wish to understand the effect of natural genetic variation on the

Proceedings of the 36th International Conference on Machine Learning, Long Beach, California, PMLR 97, 2019. Copyright 2019 by the author(s).

presence of a disease or a medical practitioner may wish to understand the effect of a patient's history on their future health. In these applications and countless others, the relative ease of modern data collection methods often yields particularly large sets of covariates for data analysts to study. While these rich data should ultimately aid understanding, they pose a number of practical challenges for data analysis. One challenge is how to discover interpretable relationships between the covariates and the outcome. Generalized linear models (GLMs) are widely used in part because they provide such interpretability – as well as the flexibility to accommodate a variety of different outcome types (including binary, count, and heavy-tailed responses). A second challenge is that, unless the number of data points is substantially larger than the number of covariates, there is likely to be non-trivial uncertainty about these relationships.

A Bayesian approach to GLM inference provides the desired coherent uncertainty quantification as well as favorable calibration properties (Dawid, 1982, Theorem 1). Bayesian methods additionally provide the ability to improve inference by incorporating expert information and sharing power across experiments. Using Bayesian GLMs leads to computational challenges, however. Even when the Bayesian posterior can be computed exactly, conjugate inference costs $O(N^2D)$ in the case of $D\gg N$. And most models are sufficiently complex as to require expensive approximations.

In this work, we propose to reduce the effective dimensionality of the feature set as a pre-processing step to speed up Bayesian inference, while still performing inference in the original parameter space; in particular, we show that low-rank descriptions of the data permit fast Markov chain Monte Carlo (MCMC) samplers and Laplace approximations of the Bayesian posterior for the full feature set. We motivate our proposal with a conjugate linear regression analysis in the case where the data are exactly low-rank. When the data are merely approximately low-rank, our proposal is an approximation. Through both theory and experiments, we demonstrate that low-rank data approximations provide a number of properties that are desirable in an efficient posterior approximation method: (1) soundness: our approximations admit error bounds directly on the quantities that practitioners report as well as practical interpretations

¹Computer Science and Artificial Intelligence Laboratory, Massachusetts Institute of Technology, Cambridge, MA ²Department of Biostatistics, Harvard, Cambridge, MA. Correspondence to: Brian L. Trippe

— Strippe @mit.edu>.

Table 1. Time complexities of naive inference and LR-GLM with a rank M approximation when $D \ge N$.

Метнор	Naive	LR-GLM	SPEEDUP
LAPLACE MCMC (ITER.)	$O(N^2D)$ O(ND)	O(NDM) $O(NM + DM)$	$N/M \ N/M$

of those bounds; (2) *tunability:* the choice of the rank of the approximation defines a tunable trade-off between the computational demands of inference and statistical precision; and (3) *conservativeness:* our approximation never reports less uncertainty than the exact posterior, where uncertainty is quantified via either posterior variance or information entropy. Together, these properties allow a practitioner to choose how much information to extract from the data on the basis of computational resources while being able to confidently trust the conclusions of their analysis.

2. Bayesian inference in GLMs

Suppose we have N data points $\{(x_n, y_n)\}_{n=1}^N$. We collect our covariates, where x_n has dimension D, in the design matrix $X \in \mathbb{R}^{N \times D}$ and our responses in the column vector $Y \in \mathbb{R}^N$. Let $\beta \in \mathbb{R}^D$ be an unknown parameter characterizing the relationship between the covariates and the response for each data point. In particular, we take β to parameterize a GLM likelihood $p(Y \mid X, \beta) = p(Y \mid X\beta)$. That is, β_d describes the effect size of the dth covariate (e.g., the influence of a non-reference allele on an individual's height in a genomic association study). Completing our Bayesian model specification, we assume a prior $p(\beta)$, which describes our knowledge of β before seeing data. Bayes' theorem gives the Bayesian posterior $p(\beta \mid Y, X) = p(\beta)p(Y \mid X\beta) / \int p(\beta')p(Y \mid X\beta')d\beta',$ which captures the updated state of our knowledge after observing data. We often summarize the β posterior via its mean and covariance. In all but the simplest settings, though, computing these posterior summaries is analytically intractable, and these quantities must be approximated.

Related work. In the setting of large D and large N, existing Bayesian inference methods for GLMs may lead to unfavorable trade-offs between accuracy and computation; see Appendix B for further discussion. While Markov chain Monte Carlo (MCMC) can approximate Bayesian GLM posteriors arbitrarily well given enough time, standard methods can be slow, with O(DN) time per likelihood evaluation. Moreover, in practice, mixing time may scale poorly with dimension and sample size; algorithms thus require many iterations and hence many likelihood evaluations. Subsampling MCMC methods can speed up inference, but they are effective only with tall data ($D \ll N$; Bardenet et al., 2017).

An alternative to MCMC is to use a deterministic approximation such as the Laplace approximation (Bishop, 2006,

Chap. 4.4), integrated nested Laplace approximation (Rue et al., 2009), variational Bayes (VB; Blei et al., 2017), or an alternative likelihood approximation (Huggins et al., 2017; Campbell & Broderick, 2019; Huggins et al., 2016). However these methods are computationally efficient only when $D \ll N$ (and in some cases also when $N \ll D$). For example, the Laplace approximation requires inverting the Hessian, which uses $O(\min(N,D)ND)$ time (Appendix C). Improving computational tractability by, for example, using a mean field approximation with VB or a factorized Laplace approximation can produce substantial bias and uncertainty underestimation (MacKay, 2003; Turner & Sahani, 2011).

A number of papers have explored using random projections and low-rank approximations in both Bayesian (Lee & Oh, 2013; Spantini et al., 2015; Guhaniyogi & Dunson, 2015; Geppert et al., 2017) and non-Bayesian (Zhang et al., 2014; Wang et al., 2017) settings. The Bayesian approaches have a variety of limitations. E.g., Lee & Oh (2013); Geppert et al. (2017); Spantini et al. (2015) give results only for certain conjugate Gaussian models. And Guhaniyogi & Dunson (2015) provide asymptotic guarantees for prediction but do not address parameter estimation.

See Section 6 for a demonstration of the empirical disadvantages of mean field VB, factored Laplace, and random projections in posterior inference.

3. LR-GLM

The intuition for our low-rank GLM (LR-GLM) approach is as follows. Supervised learning problems in highdimensional settings often exhibit strongly correlated covariates (Udell & Townsend, 2019). In these cases, the data may provide little information about the parameter along certain directions of parameter space. This observation suggests the following procedure: first identify a relatively lowerdimensional subspace within which the data most directly inform the posterior, and then perform the data-dependent computations of posterior inference (only) within this subspace, at lower computational expense. In the context of GLMs with Gaussian priors, the singular value decomposition (SVD) of the design matrix X provides a natural and effective mechanism for identifying a subspace. We will see that this perspective gives rise to simple, efficient, and accurate approximate inference procedures. In models with non-Gaussian priors the approximation enables more efficient inference by facilitating faster likelihood evaluations.

Formally, the first step of LR-GLM is to choose an integer M such that 0 < M < D. For any real design matrix X, its SVD exists and may be written as

$$X^{\top} = U \operatorname{diag}(\lambda) V^{\top} + \bar{U} \operatorname{diag}(\bar{\lambda}) \bar{V}^{\top},$$

where $U \in \mathbb{R}^{D \times M}$, $\bar{U} \in \mathbb{R}^{D \times (D-M)}$, $V \in \mathbb{R}^{N \times M}$, and $\bar{V} \in \mathbb{R}^{N \times (D-M)}$ are matrices of orthonormal rows, and

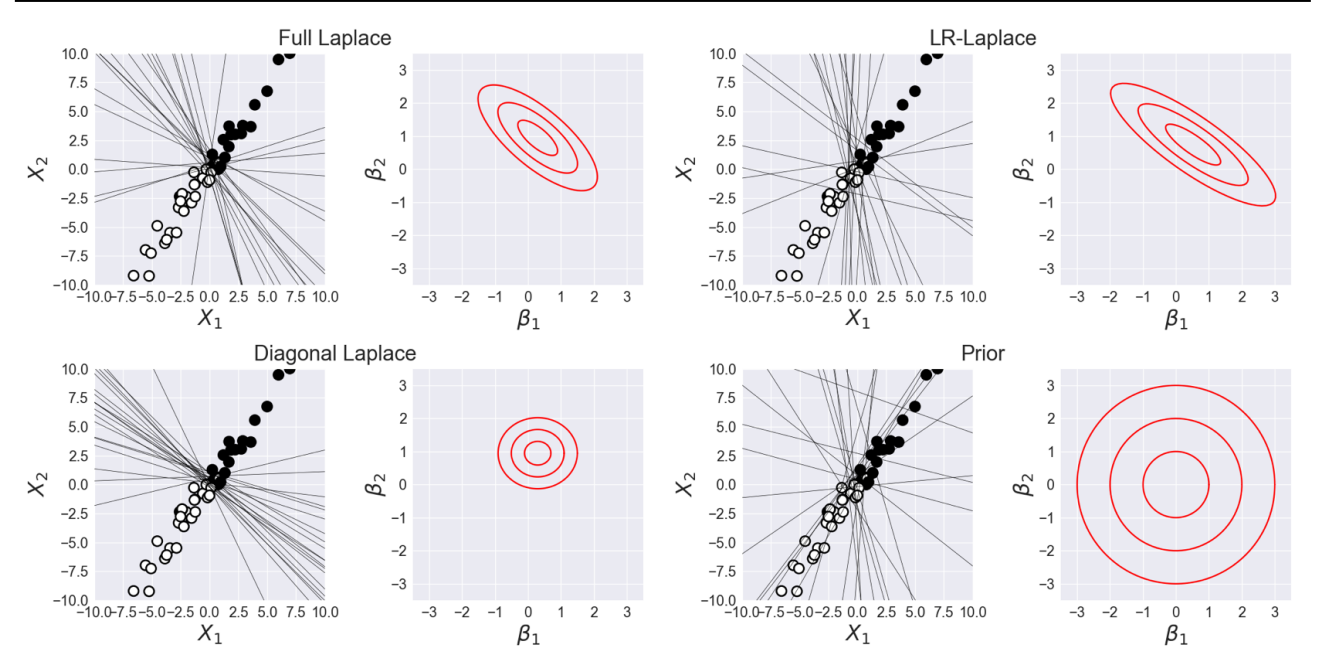


Figure 1. LR-Laplace with a rank-1 data approximation closely matches the Bayesian posterior of a toy logistic regression model. In each pair of plots, the left panel depicts the same 2-dimensional dataset with points in two classes (black and white dots) and decision boundaries (black lines) separating the two classes, which are sampled from the given posterior approximation (see title for each pair). In the right panel, the red contours represent the marginal posterior approximation of the parameter β (a bias parameter is integrated out).

 $\lambda \in \mathbb{R}^M$ and $\bar{\lambda} \in \mathbb{R}^{D-M}$ are vectors of non-increasing singular values $\lambda_1 \geq \cdots \geq \lambda_M \geq \bar{\lambda}_1 \geq \cdots \geq \bar{\lambda}_{D-M} \geq 0$. We replace X with the low-rank approximation XUU^{\top} . Note that the resulting posterior approximation $\tilde{p}(\beta \mid X, Y)$ is still a distribution over the full D-dimensional β vector:

$$\tilde{p}(\beta \mid X, Y) := \frac{p(\beta)p(Y \mid XUU^{\top}\beta)}{\int p(\beta')p(Y \mid XUU^{\top}\beta')d\beta'}$$
(1)

In this way, we cast low-rank data approximations for approximate Bayesian inference as a likelihood approximation. This perspective facilitates our analysis of posterior approximation quality and provides the flexibility either to use the likelihood approximation in an otherwise exact MCMC algorithm or to make additional fast approximations such as the Laplace approximation.

We let *LR-Laplace* denote the combination of LR-GLM and the Laplace approximation. Figure 1 illustrates LR-Laplace on a toy problem and compares it to full Laplace, the prior, and diagonal Laplace. Diagonal Laplace refers to a factorized Laplace approximation in which the Hessian of the log posterior is approximated with only its diagonal. While this example captures some of the essence of our proposed approach, we emphasize that our focus in this paper is on problems that are high-dimensional.

4. Low-rank data approximations for conjugate Gaussian regression

We now consider the quality of approximate Bayesian inference using our LR-GLM approach in the case of conjugate Gaussian regression. We start by assuming that the data is exactly low rank since it most cleanly illustrates the computational gains from LR-GLM. We then move on to the case of conjugate regression with approximately low-rank data and rigorously characterize the quality of our approximation via interpretable error bounds. We consider non-conjugate GLMs in Section 5. We defer all proofs to the Appendix.

4.1. Conjugate regression with exactly low-rank data

Classic linear regression fits into our GLM likelihood framework with $p(Y|X,\beta) = \mathcal{N}(Y|X\beta,(\tau I_N)^{-1})$, where $\tau > 0$ is the precision and I_N is the identity matrix of size N. For the conjugate prior $p(\beta) = \mathcal{N}(\beta|0,\Sigma_\beta)$, we can write the posterior in closed form: $p(\beta|Y,X) = \mathcal{N}(\beta|\mu_N,\Sigma_N)$, where $\Sigma_N := (\Sigma_\beta^{-1} + \tau X^T X)^{-1}$ and $\mu_N := \tau \Sigma_N X^\top Y$.

While conjugacy avoids the cost of approximating Bayesian inference, it does not avoid the often prohibitive $O(ND^2+D^3)$ cost of calculating Σ_N (which requires computing and then inverting Σ_N^{-1}) and the $O(D^2)$ memory demands of storing it. In the $N\ll D$ setting, these costs can be mitigated by using the Woodbury formula to obtain μ_N and Σ_N in $O(N^2D)$ time with O(ND) memory (Appendix C). But this alternative becomes computationally prohibitive as well

when both N and D are large (e.g., $D \approx N > 20,000$).

Now suppose that X is rank $M \ll \min(D,N)$ and can therefore be written as $X = XUU^T$ exactly, where $U \in \mathbb{R}^{D \times M}$ denotes the top M right singular vectors of X. Then, if $\Sigma_{\beta} = \sigma_{\beta}^2 I_D$ and 1_M is the ones vector of length M, we can write (see Appendix D.1 for details)

$$\Sigma_{N} = \sigma_{\beta}^{2} \left\{ I - U \operatorname{diag} \left(\frac{\tau \lambda \odot \lambda}{\sigma_{\beta}^{-2} 1_{M} + \tau \lambda \odot \lambda} \right) U^{\top} \right\}$$
 and
$$\mu_{N} = U \operatorname{diag} \left(\frac{\tau \lambda}{\sigma_{\beta}^{-2} 1_{M} + \tau \lambda \odot \lambda} \right) V^{\top} Y,$$
 (2)

where multiplication (\odot) and division in the diag input are component-wise across the vector λ . Eq. (2) provides a more computationally efficient route to inference. The singular vectors in U may be obtained in $O(ND\log M)$ time via a randomized SVD (Halko et al., 2011) or in O(NDM) time using more standard deterministic methods (Press et al., 2007). The bottleneck step is finding λ via $\operatorname{diag}(\lambda \odot \lambda) = U^{\top}X^{\top}XU$, which can be computed in O(NDM) time. As for storage, this approach requires keeping only U, λ , and $V^{\top}Y$, which takes just O(MD) space. In sum, utilizing low-rank structure via Eq. (2) provides an order $\min(N,D)/M$ -fold improvement in both time and memory over more naive inference.

4.2. Conjugate regression with low-rank approximations

While the case with exactly low-rank data is illustrative, real data are rarely exactly low rank. So, more generally, LR-GLM will yield an approximation $\mathcal{N}(\beta|\tilde{\mu}_N,\tilde{\Sigma}_N)$ to the posterior $\mathcal{N}(\beta|\mu_N,\Sigma_N)$, rather than the exact posterior as in Section 4.1. We next provide upper bounds on the error from our approximation. Since practitioners typically report posterior means and covariances, we focus on how well LR-GLM approximates these functionals.

Theorem 4.1. For conjugate Bayesian linear regression, the LR-GLM approximation Eq. (1) satisfies

$$\|\tilde{\mu}_{N} - \mu_{N}\|_{2} \leq \frac{\bar{\lambda}_{1}(\bar{\lambda}_{1}\|\bar{U}^{\top}\tilde{\mu}_{N}\|_{2} + \|\bar{V}^{\top}Y\|_{2})}{\|\tau\Sigma_{\beta}\|_{2}^{-1} + \bar{\lambda}_{D-M}^{2}}$$
(3)

and
$$\Sigma_N^{-1} - \tilde{\Sigma}_N^{-1} = \tau (X^{\top} X - U U^{\top} X^{\top} X U U^{\top}).$$
 (4)

In particular,
$$\|\Sigma_N^{-1} - \tilde{\Sigma}_N^{-1}\|_2 = \tau \bar{\lambda}_1^2$$
.

The major driver of the approximation error of the posterior mean and covariance is $\bar{\lambda}_1 = \|X - XUU^\top\|_2$, the largest truncated singular value of X. This result accords with the intuition that if the data are "approximately low-rank" then LR-GLM should perform well.

The following corollary shows that the posterior mean estimate is not, in general, consistent for the true parameter. But

it does exhibit reasonable asymptotic behavior. In particular, $\tilde{\mu}_N$ is consistent within the span of U and converges to the *a priori* most probable vector with this characteristic (see the toy example in Figure E.1).

Corollary 4.2. Suppose $x_n \overset{i.i.d.}{\sim} p_*$, for some distribution p^* , and $y_n \mid x_n \overset{indep}{\sim} \mathcal{N}(x_n^\top \mu_*, \tau^{-1})$, for some $\mu_* \in \mathbb{R}^D$. Assume $\mathbb{E}_{p_*}[x_n x_n^\top]$ is nonsingular. Let the columns of $U_* \in \mathbb{R}^{D \times M}$ be the top eigenvectors of $\mathbb{E}_{p_*}[x_n x_n^T]$. Then $\tilde{\mu}_N$ converges weakly to the maximum a priori vector $\tilde{\mu}$ satisfying $U_*^\top \tilde{\mu} = U_*^\top \mu_*$.

In the special case that Σ_{β} is diagonal this result implies that $\tilde{\mu}_N \stackrel{\mathcal{P}}{\to} U_* U_*^{\top} \mu_*$ (Appendices E.3 and F.2). Thus Corollary 4.2 reflects the intuition that we are not learning anything about the relation between response and covariates in the data directions that we truncate away with our approach. If the response has little dependence on these directions, $\bar{U}_*\bar{U}_*^{\top}\mu_* = \lim_{N\to\infty}\tilde{\mu}_N - \mu_*$ will be small and the error in our approximation will be low (Appendix E.3). If the response depends heavily on these directions, our error will be higher. This challenge is ubiquitous in dealing with projections of high-dimensional data. Indeed, we often see explicit assumptions encoding the notion that high-variance directions in X are also highly predictive of the response (see, e.g., Zhang et al., 2014, Theorem 2).

Our next corollary captures that LR-GLM never underestimates posterior uncertainty (the *conservativeness* property).

Corollary 4.3. *LR-GLM approximate posterior uncertainty in any linear combination of parameters is no less than the exact posterior uncertainty. Equivalently,* $\tilde{\Sigma}_N - \Sigma_N$ *is positive semi-definite.*

See Figure 1 for an illustration of this result. From an approximation perspective, overestimating uncertainty can be seen as preferable to underestimation as it leads to more conservative decision-making. An alternative perspective is that we actually engender additional uncertainty simply by making an approximation, with more uncertainty for coarser approximations, and we should express that in reporting our inferences. This behavior stands in sharp contrast to alternative fast approximate inference methods, such as diagonal Laplace approximations (Appendix F.8) and variational Bayes (MacKay, 2003), which can dramatically underestimate uncertainty. We further characterize the conservativeness of LR-GLM in Corollary E.1, which shows that the LR-GLM posterior never has lower entropy than the exact posterior and quantifies the bits of information lost due to approximation.

¹This manipulation is purely symbolic. See Appendix F.1 for details.

Algorithm 1 LR-Laplace for Bayesian inference in GLMs with low-rank data approximations and zero-mean prior – with computation costs. See Appendix H for the general algorithm.

1: Input: $prior p(\beta) = \mathcal{N}(0, \Sigma_{\beta})$, data $X \in \mathbb{R}^{N,D}$, rank $M \ll N$	D, GLM mapping ϕ with ϕ'' (S	see Eq. (5) and Section 5.1)
2: Pseudo-Code	3: Time Complexity	4: Memory Complexity
5: Data preprocessing — M-Truncated SVD		
6: $U, \operatorname{diag}(\lambda), V := \operatorname{truncated-SVD}(X^T, M)$	O(NDM)	O(NM + DM)
7: Optimize in projected space and find approximate MAP estimate	ate	
8: $\gamma_* := \arg \max_{\gamma \in \mathbb{R}^M} \sum_{i=1}^N \phi(y_i, x_i U \gamma) - \frac{1}{2} \gamma^\top U^\top \Sigma_\beta U \gamma$	$O(NM + DM^2)$	$O(N+M^2)$
9: $\hat{\mu} = U\gamma_* + \bar{U}\bar{U}^{\dagger}\Sigma_{\beta}\bar{U}(\bar{U}^{\dagger}\Sigma_{\beta}U)^{-1}\gamma_*$	O(DM)	O(DM)
10: Compute approximate posterior covariance		
11: $W^{-1} := U^{\top} \Sigma_{\beta} U - (U^{\top} X^{\top} \operatorname{diag}(\vec{\phi}''(Y, XUU^{\top} \hat{\mu})) XU)^{-1}$	$O(NM^2 + DM)$	O(NM)
$12: \ \hat{\Sigma} := \Sigma_{\beta} - \Sigma_{\beta} U W U^{\top} \Sigma_{\beta}$	0 (see footnote ¹)	O(DM)
13: Compute variances and covariances of parameters		
14: $\operatorname{Var}_{\hat{p}}(\beta_i) = e_i^{\top} \hat{\Sigma} e_i$	$O(M^2)$	O(DM)
15: $\operatorname{Cov}_{\hat{p}}(\beta_i, \beta_j) = e_i^{\top} \hat{\Sigma} e_j$	$O(M^2)$	O(DM)

5. Non-conjugate GLMs with approximately low-rank data

While the conjugate linear setting facilitates intuition and theory, GLMs are a larger and more broadly useful class of models for which efficient and reliable Bayesian inference is of significant practical concern. Assuming conditional independence of the observations given the covariates and parameter, the posterior for a GLM likelihood can be written

$$\log p(\beta \mid X, Y) = \log p(\beta) + \sum_{n=1}^{N} \phi(y_n, x_n^{\top} \beta) + Z \quad (5)$$

for some real-valued mapping function ϕ and log normalizing constant Z. For priors and mapping functions that do not form a conjugate pair, accessing posterior functionals of interest is analytically intractable and requires posterior approximation. One possibility is to use a Monte Carlo method such as MCMC, which has theoretical guarantees asymptotic in running time but is relatively slow in practice. The usual alternative is a deterministic approximation such as VB or Laplace. These approximations are typically faster but do not become arbitrarily accurate in the limit of infinite computation. We next show how LR-GLM can be applied to facilitate faster MCMC samplers and Laplace approximations for Bayesian GLMs. We also characterize the additional error introduced to Laplace approximations by low-rank data approximations.

5.1. LR-GLM for fast Laplace approximations

The Laplace approximation refers to a Gaussian approximation obtained via a second-order Taylor approximation of the log density. In the Bayesian setting, the Laplace ap-

proximation $\bar{p}(\beta \mid X,Y)$ is typically formed at the maximum a posteriori (MAP) parameter: $\bar{p}(\beta \mid X,Y):=\mathcal{N}(\beta \mid \bar{\mu},\bar{\Sigma}),$ where $\bar{\mu}:=\arg\max_{\beta}\log p(\beta \mid X,Y)$ and $\bar{\Sigma}^{-1}:=-\nabla_{\beta}^{2}\log p(\beta \mid X,Y)|_{\beta=\bar{\mu}}.$ When computing and analyzing Laplace approximations for GLMs, we will often refer to vectorized first, second, and third derivatives $\bar{\phi}',\bar{\phi}'',\bar{\phi}'''\in\mathbb{R}^{N}$ of the mapping function ϕ . For $Y,A\in\mathbb{R}^{N},$ we define $\bar{\phi}'(Y,A)_{n}:=\frac{\partial}{\partial a}\phi(Y_{n},a)|_{a=A_{n}}.$ The higher-order derivative definitions are analogous, with the derivative order of $\frac{\partial}{\partial a}$ increased commensurately.

Laplace approximations are typically much faster than MCMC for moderate/large N and small D, but they become expensive or intractable for large D. In particular, they require inverting a $D \times D$ Hessian matrix, which is in general an $O(D^3)$ time operation, and storing the resulting covariance matrix, which requires $O(D^2)$ memory.²

As in the conjugate case, LR-GLM permits a faster and more memory-efficient route to inference. Here, we say that the *LR-Laplace approximation*, $\hat{p}(\beta \mid X,Y) = \mathcal{N}(\beta \mid \hat{\mu},\hat{\Sigma})$, denotes the Laplace approximation to the LR-GLM approximate posterior. The special case of LR-Laplace with zero-mean prior is given in Algorithm 1 as it allows us to easily analyze time and memory complexity. For the more general LR-Laplace algorithm, see Appendix H.

Theorem 5.1. In a GLM with a zero-mean, structured-Gaussian prior³ and a log-concave likelihood,⁴ the rank-

 $^{^2}$ Notably, as in the conjugate setting, an alternative matrix inversion using the Woodbury identity reduces this cost when N < D to $O(N^2D)$ time and O(ND) memory (Appendix C).

³For example (banded) diagonal or diagonal plus low-rank, such that matrix vector multiplies may be computed in O(D) time.

⁴This property is standard for common GLMs such as logistic

M LR-Laplace approximation may be computed via Algorithm 1 in O(NDM) time with O(DM + NM) memory. Furthermore, any posterior covariance entry can be computed in $O(M^2)$ time.

Algorithm 1 consists of three phases: (1) computation of the M-truncated SVD of X^{\top} ; (2) MAP optimization to find $\hat{\mu}$; and (3) estimation of $\hat{\Sigma}$. In the second phase we are able to efficiently compute $\hat{\mu}$ by first solving a lower-dimensional optimization for the quantity $\gamma_* \in \mathbb{R}^M$ (Line 8), from which $\hat{\mu}$ is available analytically. Notably, in the common case that $p(\beta)$ is isotropic Gaussian, the expression for $\hat{\mu}$ reduces to $U\gamma_*$ and the full time complexity of MAP estimation is O(NM+DM). Though computing the covariance for each pair of parameters and storing $\hat{\Sigma}$ explicitly would of course require a potentially unacceptable $O(D^2)$ storage, the output of Algorithm 1 is smaller and enables arbitrary parameter variances and covariances to be computed in $O(M^2)$ time. See Appendix F.1 for additional details.

5.2. Accuracy of the LR-Laplace approximation

We now consider the quality of the LR-Laplace approximate posterior relative to the usual Laplace approximation. Our first result concerns the difference of the posterior means

Theorem 5.2 (Non-asymptotic). In a generalized linear model with an α -strongly log concave posterior, the exact and approximate MAP values, $\hat{\mu} = \arg \max_{\beta} \tilde{p}(\beta \mid X, Y)$ and $\bar{\mu} = \arg \max_{\beta} p(\beta \mid X, Y)$, satisfy

$$\|\hat{\mu} - \bar{\mu}\|_2 \leq \frac{\bar{\lambda}_1 \left(\|\vec{\phi}'(Y, X \hat{\mu})\|_2 + \lambda_1 \|\bar{U}^\top \hat{\mu}\|_2 \|\vec{\phi}''(Y, A)\|_\infty \right)}{\alpha}$$

for some vector $A \in \mathbb{R}^N$ such that $A_n \in [x_n^\top U U^\top \hat{\mu}, x_n^\top \hat{\mu}]$.

This bound reveals several characteristics of the regimes in which LR-Laplace performs well. As in conjugate regression, we see that the bound tightens to 0 as the rank of the approximation increases to capture all of the variance in the covariates and $\bar{\lambda}_1 \to 0$.

Remark 5.3. For many common GLMs, $\|\vec{\phi}'\|_2$, $\|\vec{\phi}''\|_{\infty}$, and $\|\vec{\phi}'''\|_{\infty}$ are well controlled; see Appendix F.4. $\|\vec{\phi}'''\|_{\infty}$ appears in an upcoming corollary.

Remark 5.4. The α -strong log concavity of the posterior is satisfied for any strongly log concave prior (e.g., a Gaussian, in which case we have $\alpha \geq \|\Sigma_{\beta}\|_2^{-1}$) and $\phi(y,\cdot)$ is concave for all y. In this common case, Theorem 5.2 provides a computable upper bound on the posterior mean error.

Remark 5.5. In contrast to the conjugate case (Corollary 4.2), general LR-GLM parameter estimates are not necessarily consistent within the span of the projection. That is, $U^{\top}\hat{\mu}_N$ may not converge to $U^{\top}\beta$ (see Appendix F.5).

and Poisson regression.

We next consider the distance between our approximation and target posterior under a Wasserstein metric (Villani, 2008). Let $\Gamma(\hat{p}, \bar{p})$ be the set of all couplings of distributions \hat{p} and \bar{p} , i.e. joint distributions $\gamma(\cdot, \cdot)$ satisfying $\hat{p}(\beta) = \int \gamma(\beta, \beta') d\beta'$ and $\bar{p}(\beta) = \int \gamma(\beta', \beta) d\beta'$ for all β . Then the 2-Wasserstein distance between \hat{p} and \bar{p} is defined

$$W_2(\hat{p}, \bar{p}) = \inf_{\gamma \in \Gamma(\hat{p}, \bar{p})} \mathbb{E}_{\gamma}[\|\hat{\beta} - \bar{\beta}\|_2^2]^{\frac{1}{2}}.$$
 (6)

Wasserstein bounds provide tight control of many functionals of interest, such as means, variances, and standard deviations (Huggins et al., 2018). For example, if $\xi_i \sim q_i$ for any distribution q_i (i=1,2), then $|\mathbb{E}[\xi_1] - \mathbb{E}[\xi_2]| \leq W_2(q_1,q_2)$ and $|\mathrm{Var}[\xi_1]^{\frac{1}{2}} - \mathrm{Var}[\xi_2]^{\frac{1}{2}}| \leq 2W_2(q_1,q_2)$.

We provide a finite-sample upper bound on the 2-Wasserstein distance between the Laplace and LR-Laplace approximations. In particular, the 2-Wasserstein will decrease to 0 as the rank of the LR-Laplace approximation increases since the largest truncated singular value $\bar{\lambda}_1$ will approach zero.

Corollary 5.6. Assume the prior $p(\beta)$ is Gaussian with covariance Σ_{β} and the mapping function $\phi(y,a)$ has bounded 2nd and 3rd derivatives with respect to a. Take A and α as in Theorem 5.2. Then $\bar{p}(\beta)$ and $\hat{p}(\beta)$ satisfy

$$W_{2}(\hat{p}, \bar{p}) \leq \sqrt{2}\bar{\lambda}_{1} \|\bar{\Sigma}\|_{2} \left\{ c \left[\|\Sigma_{\beta}^{-1}\|_{2} + (\lambda_{1} + \bar{\lambda}_{1})^{2} \|\vec{\phi}''\|_{\infty} \right] + \left[\lambda_{1}^{2} r + (\bar{\lambda}_{1} + 2\lambda_{1}) \|\vec{\phi}''\|_{\infty} \right] \sqrt{\operatorname{tr}(\hat{\Sigma})} \right\}, (7)$$

where
$$c := (\|\vec{\phi}'(Y, X\hat{\mu})\|_2 + \lambda_1 \|\bar{U}^{\top}\hat{\mu}\|_2 \|\vec{\phi}''(Y, A)\|_{\infty})/\alpha$$

and $r := \|U^{\top}\hat{\mu}\|_{\infty} \|\vec{\phi}'''\|_{\infty} + \lambda_1 c \|\vec{\phi}'''\|_{\infty}$.

When combined with Huggins et al. (2018, Prop. 6.1), this result guarantees closeness in 2-Wasserstein of LR-Laplace to the exact posterior.

We conclude with a result showing that the error due to the LR-GLM approximation cannot grow without bound as the sample size increases.

Theorem 5.7 (Asymptotic). Under mild regularity conditions, the error in the posterior means, $\|\hat{\mu}_n - \bar{\mu}_n\|_2$, converges as $n \to \infty$, and the limit is finite almost surely.

For the formal statement see Theorem F.2 in Appendix F.7.

5.3. LR-MCMC for faster MCMC in GLMs

LR-Laplace is inappropriate when the posterior is poorly approximated by a Gaussian. This may be the case, for example, when the posterior is multi-modal, a common characteristic of GLMs with sparse priors. To remedy this limitation of LR-Laplace, we introduce *LR-MCMC*, a wrapper around the Metropolis–Hastings algorithm using the LR-GLM approximation. For a GLM, each full likelihood and gradient

computation takes O(ND) time but only O(NM+DM) time with the LR-GLM approximation, resulting in the same $\min(N,D)/M$ -fold speedup obtained by LR-Laplace. See Appendix G for further details on LR-MCMC.

6. Experiments

We empirically evaluated LR-GLM on real and synthetic datasets. For synthetic data experiments, we considered logistic regression with covariates of dimension D=250 and D=500. In each replicate, we generated the latent parameter from an isotropic Gaussian prior, $\beta \sim \mathcal{N}(0,I_D)$, correlated covariates from a multivariate Gaussian, and responses from the logistic regression likelihood (see Appendix A.1 for details). We compared to the standard Laplace approximation, the diagonal Laplace approximation, the Laplace approximation with a low-rank data approximation obtained via random projections rather than the SVD ("Random-Laplace"), and mean-field automatic differentiation variational inference in Stan (ADVI-MF).⁵

Computational–statistical trade-offs. Figure 2A shows empirically the tunable computational–statistical trade-off offered by varying M in our low-rank data approximation. This plot depicts the error in posterior mean and variance estimates relative to results from the No-U-Turn Sampler (NUTS) in Stan (Hoffman & Gelman, 2014; Carpenter et al., 2017), which we treat as ground truth. As expected, LR-Laplace with larger M takes longer to run but yields lower errors. Random-Laplace was usually faster but provided a poor posterior approximation. Interestingly, the error of the Random-Laplace approximate posterior mean actually increased with the dimension of the projection. We conjecture this behavior may be due to Random-Laplace prioritizing covariate directions that are correlated with directions where the parameter, β , is large.

We also consider predictive performance via the classification error rate and the average negative log likelihood. In particular, we generated a *test* dataset with covariates drawn from the same distribution as the observed dataset and an *out-of-sample* dataset with covariates drawn from a different distribution (see Appendix A.1). The computation time vs. performance trade-offs, presented in Figure A.1 on the test and out-of-sample datasets, mirror the results for approximating the posterior mean and variances. In this evaluation, correctly accounting for posterior uncertainty appears less important for in-sample prediction. But in the out-of-sample case, we see a dramatic difference in negative log likelihood. Notably, ADVI-MF and diagonal Laplace exhibit much worse performance. These results support the

utility of correctly estimating Bayesian uncertainty when making out-of-sample predictions.

Conservativeness. A benefit of LR-GLM is that the posterior approximation never underestimates the posterior uncertainty (see Corollary 4.3). Figure 2C illustrates this property for LR-Laplace applied to logistic regression. When LR-Laplace misestimates posterior variances, it always overestimates. Also, when LR-Laplace misestimates means (Figure A.2), the estimates shrink closer to the prior mean, zero in this case. These results suggest that LR-GLM interpolates between the exact posterior and the prior. Notably, this property is not true of all methods. The diagonal Laplace approximation, by contrast, dramatically underestimates posterior marginal variances (see Appendix F.8).

Reliability and calibration. Bayesian methods enjoy desirable calibration properties under correct model specification. But since LR-Laplace serves as a likelihood approximation, it does not retain this theoretical guarantee. Therefore, we assessed its calibration properties empirically by examining the credible sets of both parameters and predictions. We found that the parameter credible sets of LR-Laplace are extremely well calibrated for all values of M between 20 and 400 (Figure 2B and Figure A.4). The prediction credible sets were well calibrated for all but the smallest value of M tested (M=20); in the M=20 case, LR-Laplace yielded under-confident predictions (Figure A.5). The good calibration of LR-Laplace stood in sharp contrast to the diagonal Laplace approximation and ADVI-MF. Random-Laplace also provided inferior calibration (Figures A.4 and A.5).

LR-GLM with MCMC and non-Gaussian priors. In Section 5.3 we argued that LR-GLM speeds up MCMC for GLMs by decreasing the cost of likelihood and gradient evaluations in black-box MCMC routines. We first examined LR-MCMC with NUTS using Stan on the same synthetic datasets as we did for LR-Laplace. In Figures A.3 and A.6, we see a similar conservativeness and computational–statistical trade-off as for LR-Laplace, and superior performance relative to alternative methods.

We expect MCMC to yield high-quality posterior approximations across a wider range of models than Laplace approximations. For example, for multimodal posteriors and other posteriors that deviate substantially from Gaussianity. We next demonstrate that LR-MCMC is useful in these more general cases. In high-dimensional settings, practitioners are often interested in identifying a sparse subset of parameters that significantly influence responses. This belief may be incorporated in a Bayesian setting through a sparsity-inducing prior such as the spike and slab prior or the horseshoe (George & McCulloch, 1993; Carvalho et al., 2009). However, posteriors in these cases may be multimodal, and scalable Bayesian inference with such priors is a challenging, active area of research (Guan & Stephens,

⁵We also tested ADVI using a full rank Gaussian approximation but found it to provide near uniformly worse performance compared to ADVI-MF. So we exclude full-rank ADVI from the presented results.

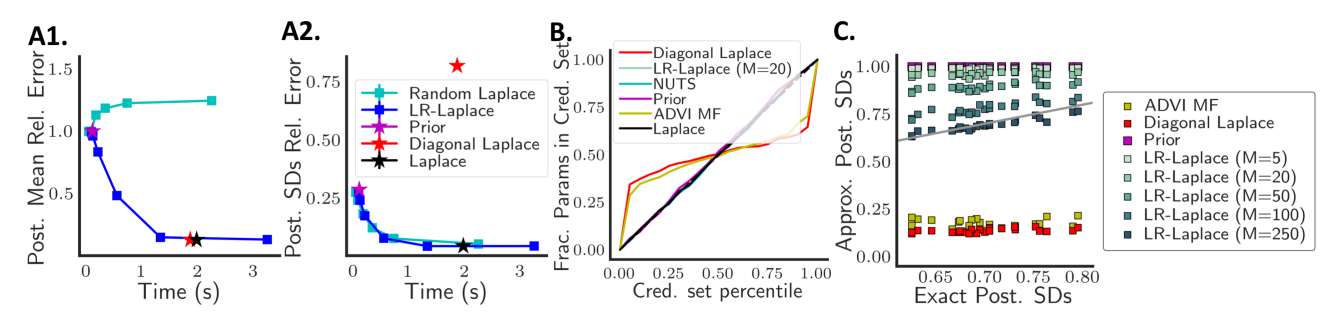


Figure 2. Left: Error of the approximate posterior (A1.) mean and (A2.) variances relative to ground truth (running NUTS with Stan). Lower and further left is better. Right (B.): Credible set calibration across all parameters and repeated experiments. (C.): Approximate posterior standard deviations for a subset of parameters. The grey line reflects zero error.

2011; Yang et al., 2016; Johndrow et al., 2017). To demonstrate the applicability of low-rank data approximations to this setting, we ran NUTS using Stan on a logistic regression model with a regularized horseshoe prior (Carvalho et al., 2009; Piironen & Vehtari, 2017). In Figure A.7, we see an attractive trade-off between computational investment and approximation error. For example, we obtained relative mean and standard deviation errors of only about 10^{-2} while reducing computation time by a factor of three.

We also applied LR-MCMC to linear regression with the regularized horseshoe prior on a dataset with very correlated covariates and D=6,238. However, this sampler exhibited severe mixing problems, both with and without the approximation, as diagnosed by large \hat{R} values in pyStan. These issues reflect the innate challenges of high-dimensional Bayesian inference with the horseshoe prior and correlated covariates.

Scalability to large-scale real datasets. Finally, we explored the applicability of LR-Laplace to two real, large-scale logistic regression tasks (Figure 3). The first is the UCI Farm-Ads dataset, which consists of N=4,143 online advertisements for animal-related topics together with binary labels indicating whether the content provider approved of the ad; there are D=54,877 bag-of-words features per ad (Dheeru & Karra Taniskidou, 2017). As with the synthetic datasets, we evaluated the error in the approximations of posterior means and variances. As a baseline to evaluate this error, we use the usual Laplace approximation because the computational demands of MCMC preclude the possibility of using it as a baseline.

As a second real dataset we evaluated our approach on the Reuters RCV1 text categorization test collection (Amini et al., 2009; Chang & Lin, 2011). RCV1 consists of D=47,236 bag-of-words features for N=20,241 English documents grouped into two different categories. We were unable to compare to the full Laplace approximation due to the high-dimensionality, so we used LR-Laplace with M=20,000 as a baseline. For both datasets, we find that as we

increase the rank of the data approximation, we incur longer running times but reduced errors in posterior means and variances. Laplace and Diagonal Laplace do not provide the same computation—accuracy trade-off.

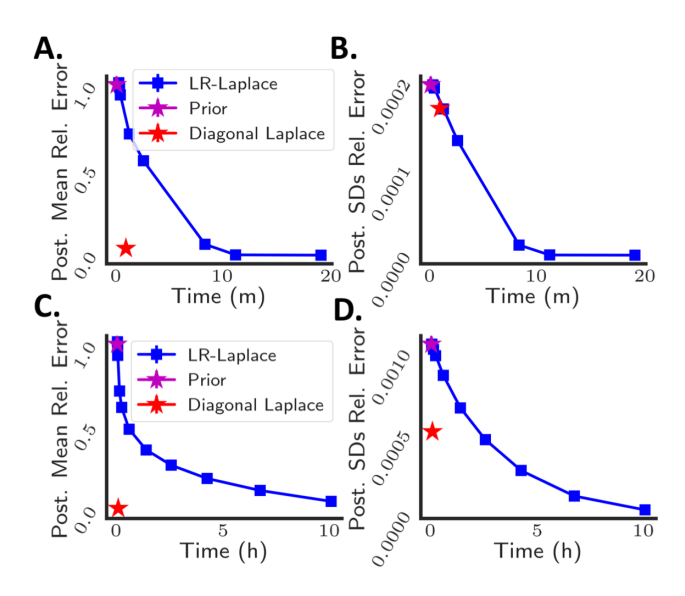


Figure 3. LR-Laplace approximation quality on Farm-Ads (top) and RCV-1 (bottom) datasets with varying M. (A.) Farm-Ads error in the posterior mean and (B.) Farm-Ads error in posterior variances (C.) RCV-1 error in posterior mean and (D.) RCV-1 error in posterior variances.

Choosing M. Applying LR-GLM requires choosing the rank M of the low rank approximation. As we have shown, this choice characterizes a computational–statistical trade-off whereby larger M leads to linearly larger computational demands, but increases the precision of the approximation. As a practical rule of thumb, we recommend setting M to be as large as is allowable for the given application without the resulting inference becoming too slow. For our experiments with LR-Laplace, this limit was $M \approx 20,000$. For LR-MCMC, the largest manageable choice of M will be problem dependent but will typically be much smaller than 20,000.

Acknowledgments

This research is supported in part by an NSF CAREER Award, an ARO YIP Award, a Google Faculty Research Award, a Sloan Research Fellowship, and ONR. BLT is supported by NSF GRFP.

References

- Amini, M., Usunier, N., and Goutte, C. Learning from Multiple Partially Observed Views an Application to Multilingual Text Categorization. In *Advances in Neural Information Processing Systems*, pp. 28–36, 2009.
- Bardenet, R., Doucet, A., and Holmes, C. On Markov Chain Monte Carlo Methods for Tall Data. *The Journal of Machine Learning Research*, 18(1):1515–1557, 2017.
- Bishop, C. M. *Pattern Recognition and Machine Learning*. Springer, 2006.
- Blei, D. M., Kucukelbir, A., and McAuliffe, J. D. Variational inference: A review for statisticians. *Journal of the American Statistical Association*, 112(518):859–877, 2017.
- Bolley, F., Gentil, I., and Guillin, A. Convergence to Equilibrium in Wasserstein Distance for Fokker–Planck Equations. *Journal of Functional Analysis*, 263(8):2430–2457, 2012.
- Boyd, S. and Vandenberghe, L. *Convex Optimization*. Cambridge University Press, 2004.
- Cai, T. T., Zhang, C.-H., and Zhou, H. H. Optimal Rates of Convergence for Covariance Matrix Estimation. *The Annals of Statistics*, 38(4):2118–2144, 2010.
- Campbell, T. and Broderick, T. Bayesian Coreset Construction via Greedy Iterative Geodesic Ascent. In *Proceedings of the 35th International Conference on Machine Learning*, volume 80, pp. 698–706, 2018.
- Campbell, T. and Broderick, T. Automated Scalable Bayesian Inference via Hilbert Coresets. *Journal of Machine Learning Research*, 20(1):551–588, 2019.
- Carpenter, B., Gelman, A., Hoffman, M. D., Lee, D., Goodrich, B., Betancourt, M., Brubaker, M., Guo, J., Li, P., and Riddell, A. Stan: A Probabilistic Programming Language. *Journal of Statistical Software*, 76(1), 2017.
- Carvalho, C. M., Polson, N. G., and Scott, J. G. Handling Sparsity via the Horseshoe. In *Artificial Intelligence and Statistics*, pp. 73–80, 2009.

- Chang, C.-C. and Lin, C.-J. LIBSVM: A Library for Support Vector Machines. *ACM Transactions on Intelligent Systems and Technology*, 2(3):27, 2011.
- Davis, C. and Kahan, W. M. The Rotation of Eigenvectors by a Perturbation. III. *SIAM Journal on Numerical Analysis*, 7(1):1–46, 1970.
- Dawid, A. P. The Well-Calibrated Bayesian. *Journal of the American Statistical Association*, 77(379):605–610, 1982.
- Dheeru, D. and Karra Taniskidou, E. UCI Machine Learning Repository, 2017.
- George, E. I. and McCulloch, R. E. Variable Selection via Gibbs Sampling. *Journal of the American Statistical Association*, 88(423):881–889, 1993.
- Geppert, L. N., Ickstadt, K., Munteanu, A., Quedenfeld, J., and Sohler, C. Random Projections for Bayesian Regression. *Statistics and Computing*, 27(1):79–101, 2017.
- Guan, Y. and Stephens, M. Bayesian Variable Selection Regression for Genome-Wide Association Studies and Other Large-Scale Problems. *The Annals of Applied Statistics*, pp. 1780–1815, 2011.
- Guhaniyogi, R. and Dunson, D. B. Bayesian Compressed Regression. *Journal of the American Statistical Association*, 110(512):1500–1514, 2015.
- Halko, N., Martinsson, P.-G., and Tropp, J. A. Finding Structure with Randomness: Probabilistic Algorithms for Constructing Approximate Matrix Decompositions. *SIAM Review*, 53(2):217–288, 2011.
- Hastings, W. K. Monte Carlo Sampling Methods Using Markov Chains and their Applications. *Biometrika*, 57 (1), 1970.
- Hoffman, M. D. and Gelman, A. The No-U-Turn Sampler: Adaptively Setting Path Lengths in Hamiltonian Monte Carlo. *Journal of Machine Learning Research*, 15(1): 1593–1623, 2014.
- Huggins, J., Campbell, T., and Broderick, T. Coresets for Scalable Bayesian Logistic Regression. In Advances in Neural Information Processing Systems, pp. 4080–4088, 2016.
- Huggins, J., Adams, R. P., and Broderick, T. PASS-GLM: Polynomial Approximate Sufficient Statistics for Scalable Bayesian GLM Inference. In *Advances in Neural Information Processing Systems*, pp. 3611–3621, 2017.
- Huggins, J. H., Campbell, T., Kasprzak, M., and Broderick, T. Practical Bounds on the Error of Bayesian Posterior Approximations: A Nonasymptotic Approach. arXiv preprint arXiv:1809.09505, 2018.

- Johndrow, J. E., Orenstein, P., and Bhattacharya, A. Scalable MCMC for Bayes Shrinkage Priors. arXiv preprint arXiv:1705.00841, 2017.
- Lee, J. and Oh, H.-S. Bayesian Regression Based on Principal Components for High-Dimensional Data. *Journal of Multivariate Analysis*, 117:175–192, 2013.
- Luenberger, D. G. *Optimization by Vector Space Methods*. John Wiley & Sons, 1969.
- MacKay, D. J. *Information Theory, Inference and Learning Algorithms*. Cambridge University Press, 2003.
- Metropolis, N., Rosenbluth, A. W., Rosenbluth, M. N., Teller, A. H., and Teller, E. Equation of State Calculations by Fast Computing Machines. *The Journal of Chemical Physics*, 21(6):1087–1092, 1953.
- Pedregosa, F., Varoquaux, G., Gramfort, A., Michel, V., Thirion, B., Grisel, O., Blondel, M., Prettenhofer, P., Weiss, R., Dubourg, V., Vanderplas, J., Passos, A., Cournapeau, D., Brucher, M., Perrot, M., and Duchesnay, E. Scikit-learn: Machine Learning in Python. *Journal of Machine Learning*, 12:2825–2830, 2011.
- Petersen, K. B. and Pedersen, M. S. The Matrix Cookbook. *Technical University of Denmark*, 7(15):510, 2008.
- Piironen, J. and Vehtari, A. Sparsity Information and Regularization in the Horseshoe and Other Shrinkage Priors. *Electronic Journal of Statistics*, 11(2):5018–5051, 2017.
- Press, W. H., Teukolsky, S. A., Vetterling, W. T., and Flannery, B. P. *Numerical Recipes 3rd Edition: The Art of Scientific Computing*. Cambridge University Press, 2007.
- Rue, H., Martino, S., and Chopin, N. Approximate Bayesian Inference for Latent Gaussian Models by Using Integrated Nested Laplace Approximations. *Journal of the Royal Statistical Society: Series B*, 71(2):319–392, 2009.
- Schmidt, M., Le Roux, N., and Bach, F. Minimizing Finite Sums with the Stochastic Average Gradient. *Mathematical Programming*, 162(1-2):83–112, 2017.
- Spantini, A., Solonen, A., Cui, T., Martin, J., Tenorio, L., and Marzouk, Y. Optimal Low-Rank Approximations of Bayesian Linear Inverse Problems. SIAM Journal on Scientific Computing, 37(6):A2451–A2487, 2015.
- Turner, R. E. and Sahani, M. Two Problems with Variational Expectation Maximisation for Time-Series Models. *Bayesian Time Series Models*, 1(3.1):3–1, 2011.
- Udell, M. and Townsend, A. Why Are Big Data Matrices Approximately Low Rank? *SIAM Journal of Mathematical Data Science*, 2019.

- Van der Vaart, A. W. *Asymptotic Statistics*, volume 3. Cambridge University Press, 2000.
- Vershynin, R. How Close is the Sample Covariance Matrix to the Actual Covariance Matrix? *Journal of Theoretical Probability*, 25(3):655–686, 2012.
- Villani, C. *Optimal Transport: Old and New*, volume 338. Springer Science & Business Media, 2008.
- Wang, J., Lee, J. D., Mahdavi, M., Kolar, M., and Srebro, N. Sketching Meets Random Projection in the Dual: A Provable Recovery Algorithm for Big and High-Dimensional Data. *Electronic Journal of Statistics*, 11(2):4896–4944, 2017.
- Yang, Y., Wainwright, M. J., and Jordan, M. I. On the Computational Complexity of High-Dimensional Bayesian Variable Selection. *The Annals of Statistics*, 44(6):2497–2532, 2016.
- Zhang, L., Mahdavi, M., Jin, R., Yang, T., and Zhu, S. Random Projections for Classification: A Recovery Approach. *IEEE Transactions on Information Theory*, 60 (11):7300–7316, 2014.
- Zhu, C., Byrd, R. H., Lu, P., and Nocedal, J. L-BFGS-B: Fortran Subroutines for Large-Scale Bound-Constrained Optimization. ACM Transactions on Mathematical Software, 23(4):550–560, 1997.

A. Additional Experimental Details and Empirical Results

A.1. Experimental Details

For all experiments we sampled β from an isotropic Gaussian prior with unit variance. For all synthetic data results we first generated a design matrix by sampling from a zero-mean Gaussian with diagonal covariance Σ with each $\Sigma_{i,i} = 5 * 1.05^{-i}$. We then used a scikit-learn (Pedregosa et al., 2011) implementation of a randomized SVD algorithm due to Halko et al. (2011), computed from two iterations (i.e., passes through X).

To assess robustness, in all experiments we used three or more replicate experiments, defined by independently generated synthetic datasets or train/test splits as well as re-rerunning the randomized truncated SVD.

The performance of the Diagonal Laplace approximation is dependent upon the shape the exact posterior at $\beta^{\rm MAP}$. In particular, using a dataset with axis aligned covariance structure gives Diagonal Laplace an unrealistic advantage given that in most real applications we do not believe that low-rank structure will be axis aligned. As such, for all synthetic data experiments presented, we randomly generated a basis of orthonormal vectors and used this basis to rotate our the design matrix. This rotation preserves the spectral decay of the data but eliminates the axis alignment of the synthetic data.

In all experiments we consider $N=2,\!500$ training examples. We obtained results on "Out of Sample Data" (in Figures A.1 and A.5) by sampling X from an alternative distribution over covariates. Specifically, we generated these out-of-sample covariates in the manner described above, but with a different random rotation matrix.

We found MAP estimation using L-BFBS-B to be the most efficient of several available options in the scipy optimize library, and used this method in all MAP estimation and Laplace approximation experiments.

For all Bayesian predictions, we use the probit approximation to the logistic function to enable fast approximation (Bishop, 2006, Chap. 4.5).

A.2. Additional Figures

In Figure A.1 we present results on prediction performance, in term of classification error, as well as negative log likelihood, reported for "Training", "Test", and "Out of Sample Data". In Figure A.2 we report the error of LR-Laplace and Random-Laplace relative to NUTS for estimation of posterior means and variances. We see here that the estimates exhibit behavior increasingly similar to that of the prior as the rank of the approximation, M, decreases. Next, Figure A.3 depicts the same error trends for LR-MCMC using NUTS in Stan. We report calibration performance of the approximations of interest for credible sets of parameters (Figure A.4) as well as for prediction (Figure A.5).

We additionally include results analogous to those in the main text for Laplace approximations using low-rank data approximations to perform faster MCMC using NUTS with Stan (Carpenter et al., 2017), in Figure A.6. Finally, we also here provide the relative error of posterior mean and standard deviation estimation for logistic regression with a regularized horseshoe prior using the LR-MCMC approximation in Figure A.7. This experiment uses Stan for inference as well.

A.2.1. HORSESHOE LOGISTIC REGRESSION EXPERIMENT

For the logistic regression experiment using a regularized horseshoe prior we used $N=1{,}000$ data points of dimension D=200. We used ten non-zero effects, each of size 10. Our implementation of the regularized horseshoe and inference in Stan closely followed M. Betancourt's "Bayes Sparse Regression" case study. We generated covariates as described in the previous section.

A.3. Stan Model Code

First we show Stan code for Bayesian logistic regression.

```
data {
  int<lower=1> N; // # of data
  int<lower=1> D; // # of covariates
  matrix[N, D] X; // Design matrix
```

 $^{^6}$ https://betanalpha.github.io/assets/case_studies/bayes_sparse_regression.html

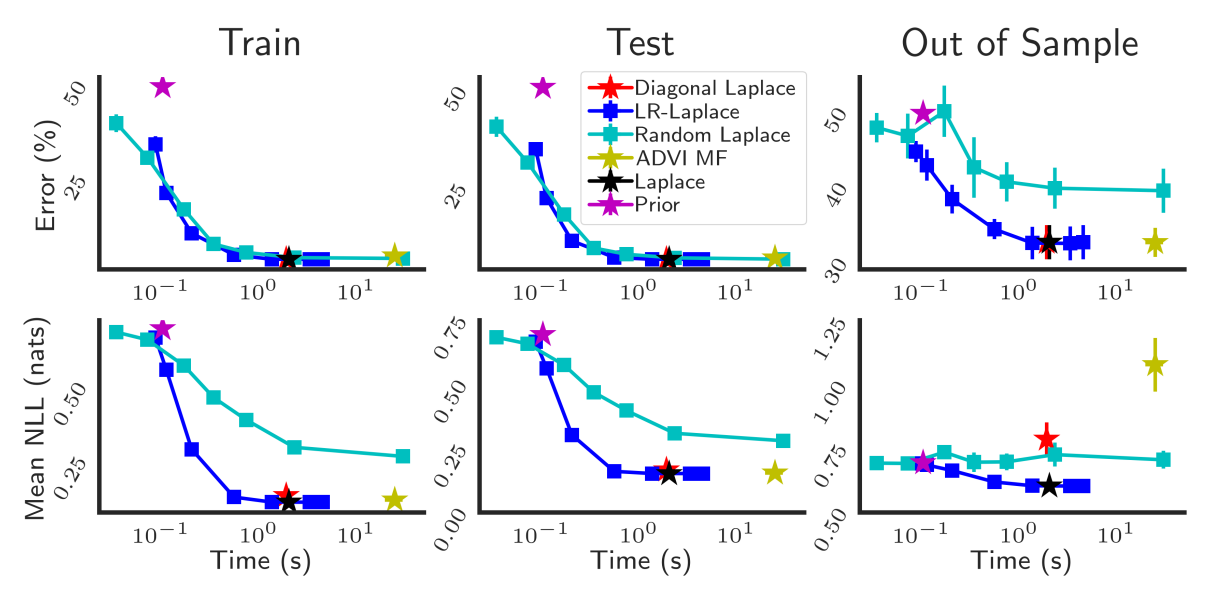


Figure A.1. Predictive performance of posterior approximations in Bayesian logistic regression in terms of (Top) classification error and (Bottom) average negative log likelihood (NLL) of responses under approximate posterior predictive distributions on (Left) *train*, (Center) *test* and (Right) *out of sample* datasets. Lower is better.

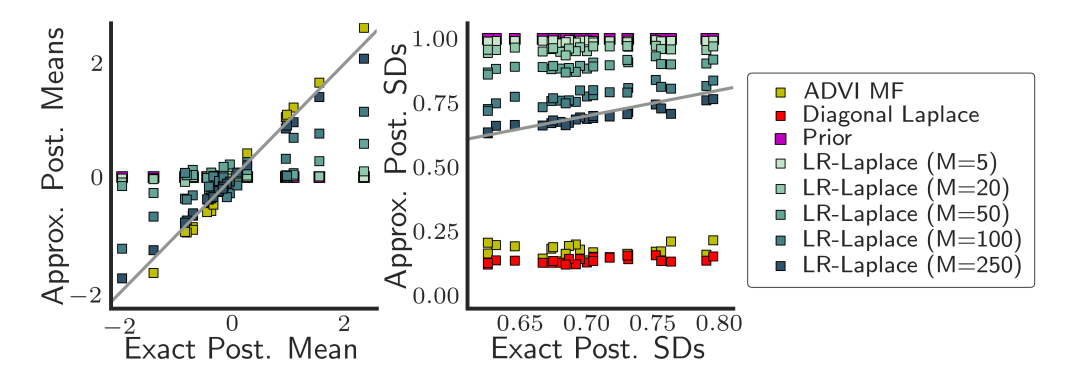


Figure A.2. Approximate posterior mean and standard deviation across a parameter subset as M varies. Horizontal axis represents ground truth from running NUTS using Stan without the LR-GLM approximation. D=250.

```
int<lower=0> y[N]; // labels
real<lower=0> sigma;
}
parameters {
  vector[D] beta;
}
model {
  beta ~ normal(0, sigma);
  y ~ bernoulli_logit(X * beta);
}
```

Second, we show Stan code for logistic regression with our low-rank approximation.

```
data {
  int<lower=1> N; // # of data
  int<lower=1> D; // # of covariates
  int<lower=1> M; // Projected dimension
```

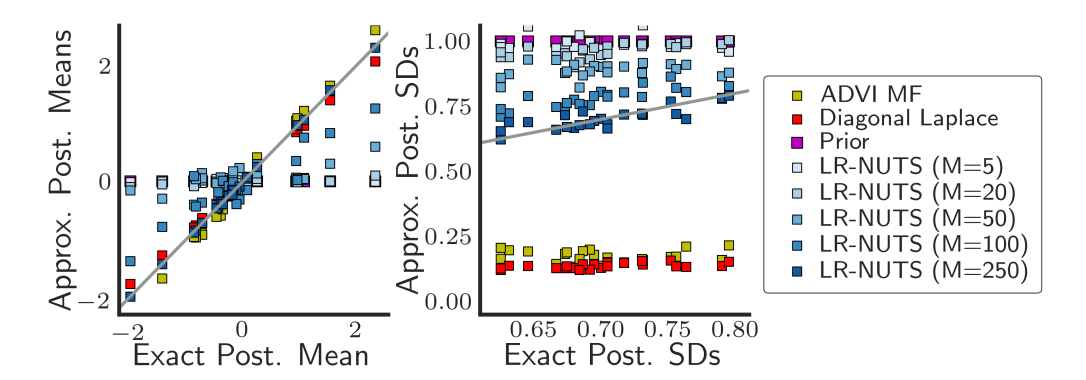


Figure A.3. This figure is analogous to Figure A.2 but examines the trade-off between computation and accuracy of LR-MCMC using NUTS in Stan. D=250.

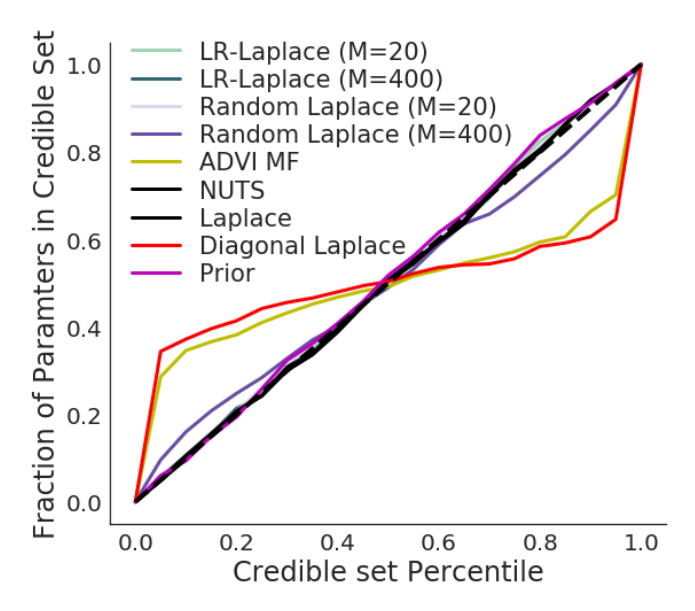


Figure A.4. Credible set calibration. The fraction of parameters in the credible sets defined by different lower tail intervals as a function of the approximate posterior probability of parameters taking values in that interval. The black dotted line (on the diagonal) reflects perfect calibration.

```
matrix[D, M] U; // Projection matrix
matrix[N, M] barX; // Projected design matrix
int<lower=0> y[N]; // labels
real<lower=0> sigma;
}
parameters {
  vector[D] beta;
}

transformed parameters {
  vector[M] bar_beta = U' * beta;
}
model {
  beta ~ normal(0, sigma);
  y ~ bernoulli_logit(barX * bar_beta);
}
```

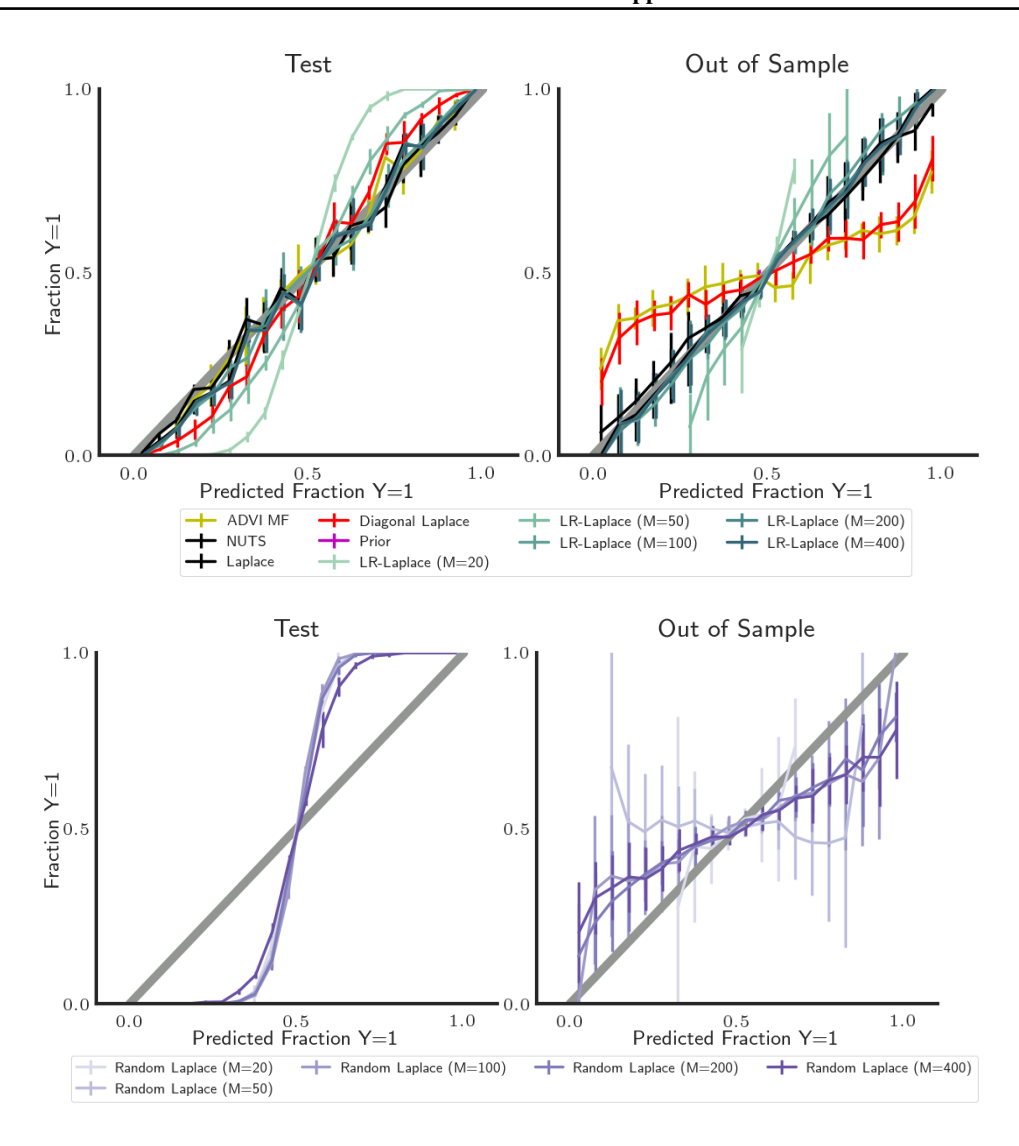


Figure A.5. Prediction calibration.

B. Related Work on Scalable Bayesian Inference

Developing scalable approximate Bayesian inference for models with many parameters (large D) and many data points (large N) has been active area of research for decades, and researchers have developed a large variety of methods applicable to GLMs. Historically, Markov chain Monte Carlo (MCMC) methods based on the Metropolis-Hastings algorithm (Metropolis et al., 1953; Hastings, 1970) have been dominant. However MCMC is computationally expensive on large-scale problems in which both D and N are very large. In particular, each likelihood evaluation requires O(DN) time, due to the matrix vector product $X\beta$. Further, estimating posterior covariances uniformly well requires $O(\log D)$ samples (Cai et al., 2010). Therefore, the total cost of collecting those samples is $O(ND\log D)$ time in the case of perfect, independent Monte Carlo samples. In practice, though, mixing times may also have unfavorable scaling with dimensionality and sample size; these issues can lead to even worse scaling in N and D. Several lines of research have explored the use of subsampling methods to reduce the dependence on N. But these methods either lose the asymptotic guarantees of exact MCMC or fail to provide faster inference in practice due to poor mixing behavior (Bardenet et al., 2017).

Other work has pursued deterministic approximations to the Bayesian posterior. Some of the most widely used of these approximations include (1) the Laplace approximation, which is a Gaussian approximation of the posterior defined locally at the posterior mode, (2) extensions of the Laplace approximation such as the integrated nested Laplace approximation (INLA)

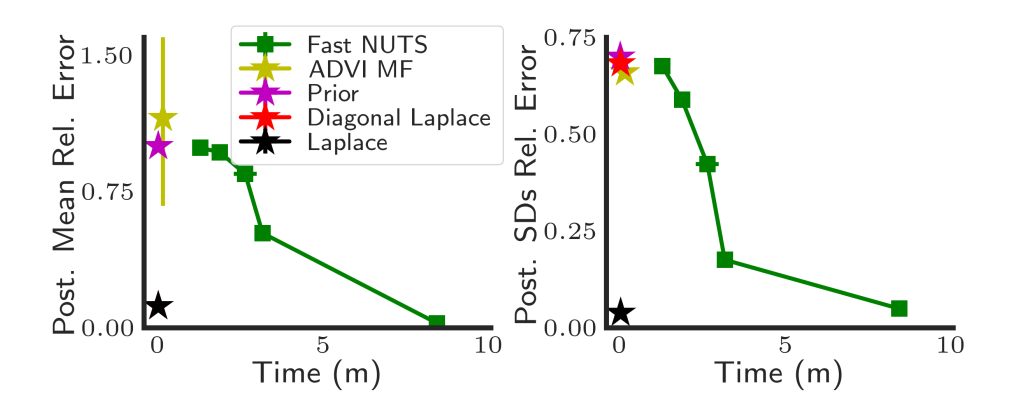


Figure A.6. This figure is analogous to Figure 2A but assesses LR-MCMC using NUTS in Stan rather than LR-Laplace. D=250.

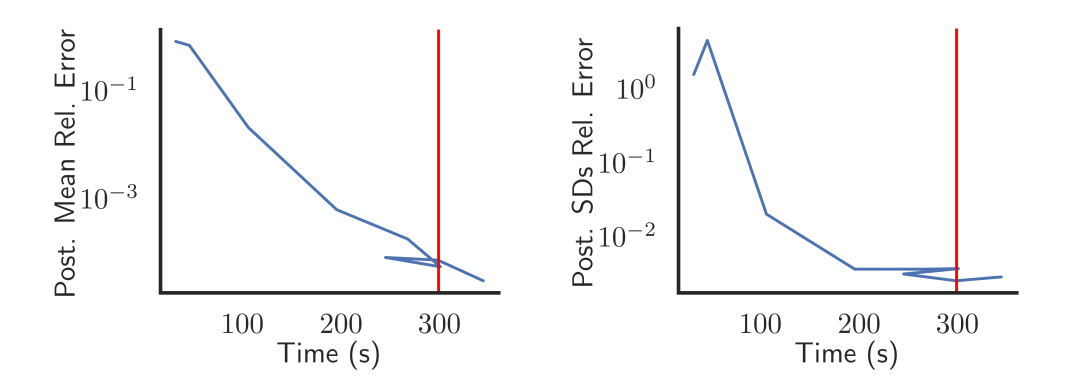


Figure A.7. Bayesian logistic regression with a regularized Horseshoe prior using NUTS in Stan. The red vertical line indicates the runtime of inference with Stan using the exact likelihood.

(Rue et al., 2009), and (3) variational Bayes; see, e.g., (Bishop, 2006, Chap. 10) and (Blei et al., 2017). However, these approaches also scale poorly with dimension in general. The Laplace approximation requires computing and inverting the Hessian of the log posterior which demand $O(ND^2)$ and $O(D^3)$ time respectively, in order to compute approximate posterior means and variances. In the $N \ll D$ setting, this cost can be reduced to $O(N^2D)$ time (Appendix C). However, in large-N settings of interest, the $O(N^2D)$ cost can be prohibitive as well. The cost of inference is further compounded when we give a fully Bayesian treatment to model hyperparameters as well as parameters; e.g., INLA requires this heavy computation for each nested approximation. In the face of difficulties posed by high dimensionality, practitioners frequently turn to factorized (or "mean-field") approximations. In the case of VB, the mean-field approach can yield biased approximations that underestimate uncertainty (MacKay, 2003; Turner & Sahani, 2011). Likewise, factorized Laplace approximations, which approximate the Hessian with only its diagonal elements, similarly underestimate uncertainty (Appendix F.8).

Some more recent work has approached scalable approximate inference in generalized linear models with theoretical guarantees on quality in the large-N regime by using likelihood approximations that are cheap to evaluate (Huggins et al., 2017; Campbell & Broderick, 2019; 2018; Huggins et al., 2016). But these methods fail to scale well to the large-D case.

More closely related to the present work, Geppert et al. (2017) and Lee & Oh (2013) focus on conjugate Bayesian regression, respectively using random projections and principle component analysis to define low-rank descriptions of the design. Lee & Oh (2013) restrict their consideration to the exactly low-rank case and primarily discuss the asymptotic consistency of the resulting posterior mean without discussing computational considerations. Spantini et al. (2015) use conjugate Bayesian regression as stepping-off point to derive a point estimator for Bayesian inverse problems. Guhaniyogi & Dunson (2015) use random projections for Bayesian GLMs but focus on predictive performance rather than parameter estimation. Outside the Bayesian context, Zhang et al. (2014), Wang et al. (2017), and many others have analyzed random projections for regression

and classification using, for example, an M-estimation framework.

C. Fast matrix inversions in the $N \ll D$ setting

In this section we focus on Gaussian conjugate linear regression with $N \ll D$. In this case, we can detail formulas for more efficient computation of the posterior mean and covariance. We start from the standard expressions for the posterior mean μ_N and covariance Σ_N when the prior is mean zero with covariance Σ_β ; see Section 3 and Section 4.1 for further notation and setup of the model. These expressions are:

$$\Sigma_N^{-1} = \Sigma_\beta^{-1} + \tau X^\top X \tag{C.1}$$

$$\mu_N = \tau \Sigma_N X^\top Y. \tag{C.2}$$

Using these formulas naively in the $D \gg N$ setting is computationally expensive due to the $O(D^3)$ time cost of matrix inversion and $O(D^2)$ storage cost.

Using the Woodbury matrix identity, $(A^{-1} + UCV)^{-1} = A - AU(C^{-1} + VAU)^{-1}VA$, allows us to write $\Sigma_N = (\Sigma_{\beta}^{-1} + X^{\top}(\tau I_N)X)^{-1}$ as

$$\Sigma_N = \Sigma_\beta - \Sigma_\beta X^\top (\tau^{-1} I_N + X \Sigma_\beta X^\top)^{-1} X \Sigma_\beta. \tag{C.3}$$

Computing Σ_N via Eq. (C.3) requires only $O(DN^2)$ cost for the matrix multiplications and an $O(N^3)$ cost for the matrix inversion. The posterior mean μ_N may then be computed in O(ND) time by multiplying through by $X^\top Y$. These time costs can be significant reductions over the naive $O(D^3)$ cost when $N \ll D$.

Fast inversions for the Laplace approximation to the GLM posterior

We here show that the same approach described above may be used for the Laplace approximation in the context of Bayesian GLMs. We say that we have a GLM likelihood if we can write

$$p(Y \mid \beta, X) = \sum_{n=1}^{N} \phi(y_n, x_n^{\top} \beta)$$

for some mapping function $\phi: \mathbb{R} \times \mathbb{R} \to \mathbb{R}$. The Bayesian posterior then becomes

$$\log p(\beta \mid X, Y) = \log p(\beta) + \sum_{n=1}^{N} \phi(y_n, x_n^{\top} \beta) + Z, \tag{C.4}$$

where Z is a typically-intractable log normalizing constant.

Due to the analytic intractability of posterior inference in many common GLMs, approximations are necessary; the Laplace approximation is a particularly widely used approximation and takes the form

$$\bar{p}(\beta) = \mathcal{N}(\beta \mid \bar{\mu}, \bar{\Sigma}),$$
 (C.5)

where $\bar{\mu} := \arg\max_{\beta} \log p(\beta \mid X, Y)$ and $\bar{\Sigma} := \left(-\nabla_{\beta}^2 \log p(\beta \mid X, Y)|_{\beta = \bar{\mu}}\right)^{-1}$. However, as in the conjugate case, computing this matrix inverse naively can be expensive in the high-dimensional setting, and we are motivated to consider more computationally efficient routes to evaluate it. In settings when $N \ll D$ and when we have a Gaussian prior $p(\beta) = \mathcal{N}(\beta \mid \mu_{\beta}, \Sigma_{\beta})$, we may take an approach similar to our approach in the conjugate case. We first note

$$\nabla_{\beta}^{2} \log p(\beta \mid X, Y)|_{\beta = \bar{\mu}} = -\Sigma_{\beta}^{-1} + X^{\mathsf{T}} \operatorname{diag}(\vec{\phi}''(Y, X\bar{\mu}))X, \tag{C.6}$$

where $\vec{\phi}''(Y,A)$ is a vector in \mathbb{R}^N defined such that for any n in $1,2,\ldots,N$, $\vec{\phi}''(Y,A)_n:=\frac{d^2}{da^2}\phi(y_i,a)|_{a=A_n}$. Applying the same trick to this expression as before, we obtain

$$\bar{\Sigma}_{N} = \left(-\nabla_{\beta}^{2} \log p(\beta \mid X, Y)|_{\beta = \bar{\mu}}\right)^{-1} = \Sigma_{\beta} - \Sigma_{\beta} X^{\top} \left(\operatorname{diag}[-\vec{\phi}''(Y, X\bar{\mu})]^{-1} + X \Sigma_{\beta} X^{\top}\right)^{-1} X \Sigma_{\beta}, \tag{C.7}$$

which again can yield computational gains.

It is worth noting however that this route is more computationally efficient only when the prior covariance matrix is structured in some way that allows for fast matrix-vector and matrix-matrix multiplications. This will be the case, for example, if Σ_{β} is diagonal, block-diagonal, banded diagonal, or diagonal plus a low-rank matrix.

D. Conjugate Gaussian regression with exactly low rank design

D.1. Derivation of Eq. (2)

Here we consider the setting of conjugate Bayesian linear regression, with X exactly low rank and $\Sigma_{\beta} = \sigma_{\beta}^2 I_D$, as detailed in Section 4.1. We now derive the expressions (Eq. (2)) for the mean and covariance of the Gaussian posterior for β in this case. We suppose $X = V \operatorname{diag}(\lambda) U^{\top}$ for U, V matrices of orthonormal rows and λ a vector. The preceding equation for X will capture low rank structure when $U \in \mathbb{R}^{D \times M}$ for some M with $M \ll \min(D, N)$.

For the covariance, we start from Eq. (C.1). Then we can rewrite Σ_N as follows.

$$\Sigma_{N} = \left(\sigma_{\beta}^{-2} I_{D} + \tau X^{\top} X\right)^{-1}$$

$$= \left(\sigma_{\beta}^{-2} I_{D} + \tau U \operatorname{diag}(\lambda) V^{\top} V \operatorname{diag}(\lambda) U^{\top}\right)^{-1}$$

$$= \left(\sigma_{\beta}^{-2} I_{D} + U \operatorname{diag}(\tau \lambda \odot \lambda) U^{\top}\right)^{-1}$$

where \odot denotes component-wise multiplication, in this case across the components of the vector λ

$$= \sigma_{\beta}^2 I - \sigma_{\beta}^2 U (\operatorname{diag}(\tau \lambda \odot \lambda)^{-1} + \sigma_{\beta}^2 I_M)^{-1} U^{\top} \sigma_{\beta}^2$$

by the Woodbury matrix identity and $U^{\top}U = I_M$

$$= \sigma_{\beta}^2 I - \sigma_{\beta}^2 U \operatorname{diag} \left\{ \left(\frac{1}{\tau \lambda \odot \lambda} + \sigma_{\beta}^2 1_M \right)^{-1} \sigma_{\beta}^2 \right\} U^{\top}$$

where division within the diag input is component-wise and 1_M is the all-ones vector of length M

$$= \sigma_{\beta}^{2} \left(I_{D} - U \operatorname{diag} \left\{ \frac{\tau \lambda \odot \lambda}{\sigma_{\beta}^{-2} 1_{M} + \tau \lambda \odot \lambda} \right\} U^{\top} \right).$$

Starting from Eq. (C.2), we can rewrite the posterior mean as follows.

$$\begin{split} &\mu_N = \tau \Sigma_N X^\top Y \\ &= \tau \sigma_\beta^2 \left(I_D - U \mathrm{diag} \left\{ \frac{\tau \lambda \odot \lambda}{\sigma_\beta^{-2} 1_M + \tau \lambda \odot \lambda} \right\} U^\top \right) U \mathrm{diag}(\lambda) V^\top Y \\ &\text{from the derivation above and substituting for } X \\ &= \tau \sigma_\beta^2 \left(U - U \mathrm{diag} \left\{ \frac{\tau \lambda \odot \lambda}{\sigma_\beta^{-2} 1_M + \tau \lambda \odot \lambda} \right\} \right) \mathrm{diag}(\lambda) V^\top Y \\ &\text{since } U^\top U = I_M \\ &= \tau \sigma_\beta^2 U \left(I_M - \mathrm{diag} \left\{ \frac{\tau \lambda \odot \lambda}{\sigma_\beta^{-2} 1_M + \tau \lambda \odot \lambda} \right\} \right) \mathrm{diag}(\lambda) V^\top Y \\ &= U \mathrm{diag} \left\{ \frac{\tau \lambda}{\sigma_\beta^{-2} 1_M + \tau \lambda \odot \lambda} \right\} V^\top Y. \end{split}$$

E. Proofs and further results for conjugate Bayesian linear regression with low-rank data approximations

E.1. Proof of Theorem 4.1

Recall that for conjugate Gaussian Bayesian linear regression, the exact posterior is $p(\beta \mid X, Y) = \mathcal{N}(\beta \mid \mu_N, \Sigma_N)$, where μ_N and Σ_N are given in Eqs. (C.1) and (C.2).

Using an orthonormal projection U yields a Gaussian approximate posterior $\tilde{p}(\beta \mid X, Y) = \mathcal{N}(\beta \mid \tilde{\mu}_N, \tilde{\Sigma}_N)$. Recall from Section 3 that we obtain this approximate posterior by replacing X with XUU^{\top} . Thus, we can find $\tilde{\mu}_N$ and $\tilde{\Sigma}_N$ by

consulting Eqs. (C.1) and (C.2):

$$\tilde{\Sigma}_N^{-1} = \Sigma_\beta^{-1} + \tau U U^\top X^\top X U U^\top \tag{E.1}$$

$$\tilde{\mu}_N = \tilde{\tau} \Sigma_N U U^\top X^\top Y. \tag{E.2}$$

Upper bound on the posterior mean approximation error

We will obtain our upper bound on the error of the approximate posterior mean relative to the exact posterior mean by upper bounding the norm of the difference between the gradient of the log posterior with respect to β at the approximate posterior mean, $\tilde{\mu}_N$, and the exact posterior mean, μ_N . Together with the strong convexity of the negative log posterior, this bound will allow us to arrive at the desired upper bound on $\|\mu_N - \tilde{\mu}_N\|_2$.

First, we bound the norm of the gradient difference. To that end, the gradients of the exact log likelihood and the approximate log likelihood are given by

$$\nabla_{\beta} \log p(Y \mid X, \beta) = \nabla_{\beta} \left[-\frac{\tau}{2} (X\beta - Y)^{\top} (X\beta - Y) \right]$$
$$= -\tau (X^{\top} X\beta - X^{\top} Y)$$

and

$$\nabla_{\beta} \log \tilde{p}(Y \mid X, \beta) = \nabla_{\beta} \left[-\frac{\tau}{2} (XUU^{\top}\beta - Y)^{\top} (XUU^{\top}\beta - Y) \right]$$
$$= -\tau (UU^{\top}X^{\top}XUU^{\top}\beta - UU^{\top}X^{\top}Y).$$

We can thus upper bound the norm of the difference between the two log posteriors as follows.

$$\begin{split} & \left\| \nabla_{\beta} \log \tilde{p}(\beta \mid X, Y) - \nabla_{\beta} \log p(\beta \mid X, Y) \right\|_{2} \\ & = \left\| \nabla_{\beta} \log \tilde{p}(Y \mid X, \beta) - \nabla_{\beta} \log p(Y \mid X, \beta) \right\|_{2} \end{split}$$

since the prior is the same in both the exact and approximate model

and since the normalizing constant has no β dependence

$$\begin{split} &= \left\| -\tau \left(U U^\top X^\top X U U^\top \beta - U U^\top X^\top Y \right) + \tau \left(X^\top X \beta - X^\top Y \right) \right\|_2 \\ &= \tau \left\| \left(X^\top X - U U^\top X^\top X U U^\top \right) \beta + U U^\top X^\top Y - X^\top Y \right\|_2 \\ &= \tau \left\| \bar{U} \bar{U}^\top X^\top X \bar{U} \bar{U}^\top \beta - \bar{U} \bar{U}^\top X^\top Y \right\|_2 \end{split}$$

where \bar{U} (above) as well as $\bar{\lambda}$ and \bar{V} (below) are defined in Section 3

$$\begin{split} &= \tau \left\| \bar{U} \mathrm{diag}(\bar{\lambda} \odot \bar{\lambda}) \bar{U}^{\top} \beta - \bar{U} \mathrm{diag}(\bar{\lambda}) \bar{V}^{\top} Y \right\|_{2} \\ &\leq \tau \left(\left\| \bar{U} \mathrm{diag}(\bar{\lambda} \odot \bar{\lambda}) \bar{U}^{\top} \beta \right\|_{2} + \left\| \bar{U} \mathrm{diag}(\bar{\lambda}) \bar{V}^{\top} Y \right\|_{2} \right) \end{split}$$

by the triangle inequality

$$= \tau \left(\left\| \operatorname{diag}(\bar{\lambda} \odot \bar{\lambda}) \bar{U}^{\top} \beta \right\|_{2} + \left\| \operatorname{diag}(\bar{\lambda}) \bar{V}^{\top} Y \right\|_{2} \right)$$

since $||v||_2^2 = v^\top v$ for a vector v and $U^\top U = I_M$

$$\leq \tau \left(\left\| \operatorname{diag}(\bar{\lambda} \odot \bar{\lambda}) \right\|_{\operatorname{op}} \left\| \bar{U}^{\top} \beta \right\|_{2} + \left\| \operatorname{diag}(\bar{\lambda}) \right\|_{\operatorname{op}} \left\| \bar{V}^{\top} Y \right\|_{2} \right)$$

by definition of the operator norm in this space

$$= \tau \left(\bar{\lambda}_1^2 \| \bar{U}^\top \beta \|_2 + \bar{\lambda}_1 \| \bar{V}^\top Y \|_2 \right) \tag{E.3}$$

Second, we need a result that will let us use the strong convexity of the negative log posterior. We prove the following result in Appendix E.2.

Lemma E.1. Let f,g be twice differentiable functions mapping $\mathbb{R}^D \to \mathbb{R}$ and attaining minima at $\beta_f = \arg\min_{\beta} f(\beta)$ and $\beta_g = \arg\min_{\beta} g(\beta)$, respectively. Additionally, assume that f is α -strongly convex for some $\alpha > 0$ on the set $\{t\beta_f + (1-t)\beta_g | t \in [0,1]\}$ and that $\|\nabla_{\beta} f(\beta_g) - \nabla_{\beta} g(\beta_g)\|_2 = \|\nabla_{\beta} f(\beta_g)\|_2 \le c$. Then

$$\|\beta_f - \beta_g\|_2 \le \frac{c}{\alpha}.\tag{E.4}$$

To use the preceding result, we need a lower bound on the strong convexity constant of the negative log posterior; we now calculate such a bound. We have that μ_N and $\tilde{\mu}_N$ are the maximum a posteriori values of β under $p(\beta|X,Y,\alpha)$ and $\tilde{p}(\beta|X,Y,\alpha)$, respectively; equivalently they minimize the respective negative log of these distributions. For a matrix A, let $\lambda_{\min}(A)$ denote its minimum eigenvalue. The Hessian of the negative log posterior with respect to β is precisely $\Sigma_{\beta}^{-1} + \tau X^{\top} X$ everywhere. So the negative log posterior is α -strongly convex, where

$$\alpha = \lambda_{\min}(\Sigma_{\beta}^{-1} + \tau X^{\mathsf{T}} X) \ge \lambda_{\min}(\Sigma_{\beta}^{-1}) + \tau \lambda_{\min}(X^{\mathsf{T}} X) = \|\Sigma_{\beta}\|_{2}^{-1} + \tau \bar{\lambda}_{D-M}^{2}. \tag{E.5}$$

In the first part of the final equality above, we use that the spectral norm of a matrix inverse is equal to the reciprocal of the minimum eigenvalue of the matrix.

Now we have an upper bound on the norm of the difference in gradients of the negative log posteriors (the same as for the log posteriors, in Eq. (E.3)) and a lower bound on the strong convexity constant from Eq. (E.5). So we can apply these together with Lemma E.1 to find

$$\begin{split} \|\mu_N - \tilde{\mu}_N\|_2 &\leq \frac{\tau \left(\bar{\lambda}_1^2 \|\bar{U}^\top \tilde{\mu}_N\|_2 + \bar{\lambda}_1 \|\bar{V}^\top Y\|_2\right)}{\alpha} \\ \text{by Lemma E.1 taking } \log p(\beta|X,Y) \text{ and } \log \tilde{p}(\beta|X,Y) \\ \text{as } f \text{ and } g \text{ respectively, with } c \text{ given by Eq. (E.3)} \\ &\leq \frac{\tau \left(\bar{\lambda}_1^2 \|\bar{U}^\top \tilde{\mu}_N\|_2 + \bar{\lambda}_1 \|\bar{V}^\top Y\|_2\right)}{\|\Sigma_\beta\|_2^{-1} + \tau \bar{\lambda}_{D-M}^2} \\ \text{by Eq. (E.5)} \\ &= \frac{\bar{\lambda}_1 \left(\bar{\lambda}_1 \|\bar{U}^\top \tilde{\mu}_N\|_2 + \|\bar{V}^\top Y\|_2\right)}{\|\tau \Sigma_\beta\|_2^{-1} + \bar{\lambda}_{D-M}^2}. \end{split}$$

Notably, in the common special case that Σ_{β} is diagonal, as we saw in Section 4.1, $\tilde{\mu}_N$ will be in the span of U, and we will have that $\|\bar{U}^{\top}\tilde{\mu}_N\|_2 = 0$.

Error in Posterior Precision

The error in the precision matrices for the approximate and exact posteriors in linear regression are particularly straightforward since they do not depend on the responses, Y. In particular, we have

$$\Sigma_N^{-1} - \tilde{\Sigma}_N^{-1} = (\Sigma_\beta^{-1} + \tau X^\top X) - (\Sigma_\beta^{-1} + \tau U U^\top X^\top X U U^\top)$$
 (E.6)

$$= \tau X^{\top} X - \tau U U^{\top} X^{\top} X U U^{\top} \tag{E.7}$$

$$= \tau \bar{U} \bar{U}^{\top} X^{\top} X \bar{U} \bar{U}^{\top} \tag{E.8}$$

$$= \tau \bar{U} \operatorname{diag}(\bar{\lambda} \odot \bar{\lambda}) \bar{U}^{\top}. \tag{E.9}$$

Thus, since it is equal to the maximum eigenvalue, the spectral norm of the error in the precisions is precisely $\|\Sigma_N^{-1} - \tilde{\Sigma}_N^{-1}\|_2 = \tau \bar{\lambda}_1^2$.

E.2. Proof of Lemma E.1

By the fundamental theorem of calculus, we may write

$$\nabla_{\beta} f(\beta) = \nabla_{\beta} f(\beta_g) + \int_{t=0}^{1} (\beta - \beta_g)^{\top} \nabla_{\beta}^{2} f(t\beta + (1-t)\beta_g) dt.$$

Considering the norm of $\nabla_{\beta} f(\beta)$ and applying the triangle inequality provides that for any β in $\{t\beta_f + (1-t)\beta_q \mid t \in [0,1]\}$,

$$\|\nabla_{\beta} f(\beta)\|_{2} \ge \left\| \int_{t=0}^{1} (\beta - \beta_{g})^{\top} \nabla_{\beta}^{2} f(t\beta + (1-t)\beta_{g}) dt \right\|_{2} - \|\nabla_{\beta} f(\beta_{g})\|_{2}$$
 (E.10)

$$\geq \|\beta - \beta_g\|_2 \left\| \int_{t-0}^1 \nabla_{\beta}^2 f(t\beta + (1-t)\beta_g) dt \right\|_2 - \|\nabla_{\beta} f(\beta_g)\|_2$$
 (E.11)

$$\geq \|\beta - \beta_g\|_2 \alpha - \|\nabla_\beta f(\beta_g)\|_2. \tag{E.12}$$

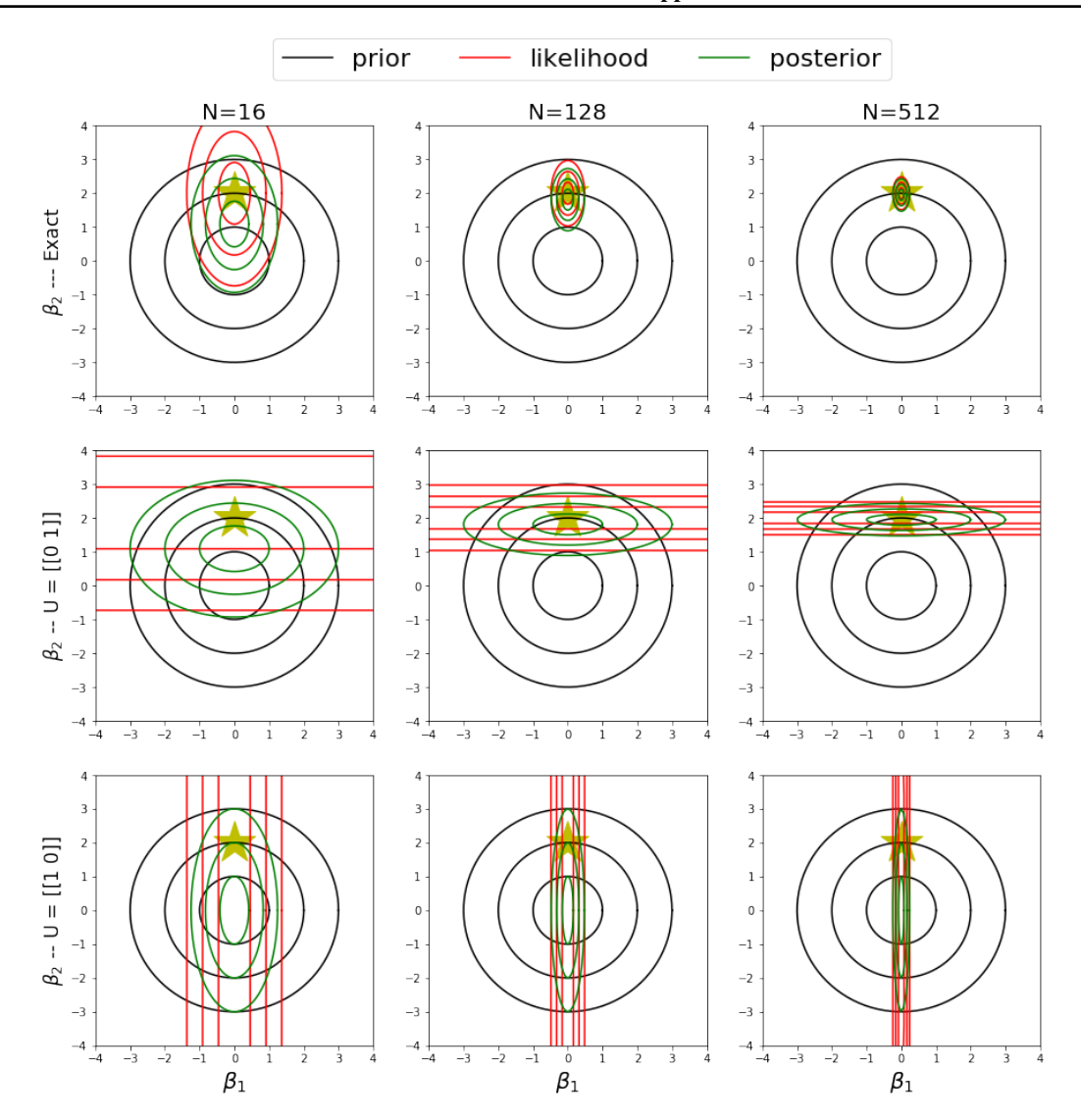


Figure E.1. Example of posterior approximations with different projections (characterized by U) for increasing sample sizes. Each plot shows the contours of three densities: the prior, likelihood, and posterior (or approximations thereof). The top row shows the exact posterior. The middle row shows the approximations found by using the best rank-1 approximation to X. The bottom row shows the approximations found using the orthogonal rank-1 approximation. The star is at the parameter value used to generate simulated data for these plots.

We consider this bound at β_f . Recall we assume that $\|\nabla_{\beta} f(\beta_g)\|_2 \le c$. And $\|\nabla_{\beta} f(\beta_f)\|_2 = 0$ since f is twice differentiable. Therefore, we have that $0 \ge \|\beta_f - \beta_g\|_2 \alpha - c$, and the result follows.

E.3. Proof of Corollary 4.2

Our approach is to show that

$$\tilde{\mu}_N \xrightarrow{p} \Sigma_{\beta} U_* (U_*^{\top} \Sigma_{\beta} U_*)^{-1} U_*^{\top} \beta. \tag{E.13}$$

We then appeal to the following result, which we prove in Appendix E.4:

Lemma E.2. $\tilde{\mu} := \Sigma_{\beta} U (U^{\top} \Sigma_{\beta} U)^{-1} U^{\top} \beta$ is the vector of minimum Σ_{β}^{-1} -norm satisfying $U^{\top} \tilde{\mu} = U^{\top} \beta$.

Finally, for any closed $S \subset \mathbb{R}^D$, $\tilde{\mu} = \arg\min_{v \in S} \|v\|_{\Sigma_{\beta}^{-1}} = \arg\max_{v \in S} -\frac{1}{2}v^{\top}\Sigma_{\beta}^{-1}v = \arg\max_{v \in S} \mathcal{N}(0, \Sigma_{\beta})$. Therefore, the $\tilde{\mu}$ in Lemma E.2 is the maximum a priori vector satisfying the constraint in Lemma E.2.

We first turn to proving Eq. (E.13). Let $U_N \operatorname{diag}(\lambda^{(N)}) V_N^{\top}$ denote the M-truncated SVD of the design matrix consisting of N samples $X = (x_1, x_2, \dots, x_N)$ where $x_i \overset{\text{i.i.d.}}{\sim} p_*$. When the low rank approximation is defined by this SVD, from Eq. (E.1) we have that $\tilde{\mu}_N = \tau \tilde{\Sigma}_N U_N U_N^{\top} X^{\top} Y$. Noting that $Y = X\beta + \frac{1}{\tau} \epsilon$ for some $\epsilon \in \mathbb{R}^N$ with $\epsilon_i \overset{\text{i.i.d.}}{\sim} \mathcal{N}(0,1)$, we may expand this out and write:

$$\begin{split} \tilde{\mu}_{N} &= \tau(\Sigma_{\beta}^{-1} + U_{N}U_{N}^{\top}X^{\top}\tau X U_{N}U_{N}^{\top})^{-1}U_{N}U_{N}^{\top}X^{\top}(X\beta + \frac{1}{\tau}\epsilon) \\ &= \tau\left\{\Sigma_{\beta}^{-1} + U_{N}\left[\tau \operatorname{diag}(\lambda^{(N)} \odot \lambda^{(N)})\right]U_{N}^{\top}\right\}^{-1}U_{N}\operatorname{diag}(\lambda^{(N)})V_{N}^{\top}\left[V_{N}\operatorname{diag}(\lambda^{(N)})U_{N}^{\top}\beta + \frac{1}{\tau}\epsilon\right] \\ &= \left\{\Sigma_{\beta}^{-1} + U_{N}\left[\tau \operatorname{diag}(\lambda^{(N)} \odot \lambda^{(N)})\right]U_{N}^{\top}\right\}^{-1}U_{N}\left[\tau \operatorname{diag}(\lambda^{(N)} \odot \lambda^{(N)})\right]\left[U_{N}^{\top}\beta + \operatorname{diag}(\lambda^{(N)})^{-1}V_{N}^{\top}\frac{1}{\tau}\epsilon\right] \\ &= \Sigma_{\beta}U_{N}\left[U_{N}^{\top}\Sigma_{\beta}U_{N} + \tau^{-1}\operatorname{diag}(\lambda^{(N)})^{-2}\right]^{-1}\left[U_{N}^{\top}\beta + \operatorname{diag}(\lambda^{(N)})^{-1}V_{N}^{\top}\frac{1}{\tau}\epsilon\right] \\ &\xrightarrow{P} \Sigma_{\beta}U_{*}(U_{*}^{\top}\Sigma_{\beta}U_{*})^{-1}U_{*}^{\top}\beta, \end{split}$$

where in the fourth line we use the matrix identity, $(R^{-1} + W^{\top}QW)^{-1}W^{\top}Q = RW^{\top}(WRW^{\top} + Q^{-1})^{-1}$ (Petersen & Pedersen, 2008). Convergence in probability in the last line follows since $\operatorname{diag}(\lambda^{(N)})^{-2} \stackrel{P}{\to} 0$ (Vershynin, 2012) and $U_N \stackrel{P}{\to} U$.

E.4. Proof of Lemma E.2

We show that $\beta_* = \Sigma_\beta U (U^\top \Sigma_\beta U)^{-1} U^\top \beta$ is the vector of minimum norm satisfying the above constraints in the Hilbert space \mathbb{R}^D with inner product $\langle v_1, v_2 \rangle = v_1^\top \Sigma_\beta^{-1} v_2$ for vectors $v_1, v_2 \in \mathbb{R}^D$.

Define β_* as

$$\beta_* = \underset{v \in \mathbb{R}^D}{\arg\min} \|v\|_{\Sigma_{\beta}^{-1}} \text{ subject to } U^{\top}v = U^{\top}\beta$$
 (E.14)

First note that the condition $U^{\top}\beta_* = U^{\top}\beta$ may be expressed as a set the M linear constraints

$$\langle \Sigma_{\beta} U[:,i], \beta_* \rangle = U[:,i]^{\top} \beta \tag{E.15}$$

for $i=1,2,\ldots,M$. We thereby see that the constraint restricts β_* to the linear variety $\beta+\left[\left\{\Sigma_\beta U[:,i]\right\}_{i=1}^M\right]^\perp$, where $\left[A\right]$ denotes the subspace generated by the vectors of the set A and $\left[A\right]^\perp$ denotes the set of all vectors orthogonal to $\left[A\right]$ (i.e. the orthogonal complement of $\left[A\right]$). By the projection theorem (Luenberger, 1969), β_* is orthogonal to $\left[\left\{\Sigma_\beta U[:,i]\right\}_{i=1}^M\right]^\perp$, or $\beta_*\in\left[\left\{\Sigma_\beta U[:,i]\right\}_{i=1}^M\right]^\perp=\left[\left\{\Sigma_\beta U[:,i]\right\}_{i=1}^M\right]$. We can therefore write β_* as a linear combination of the vectors $\left\{\Sigma_\beta U[:,i]\right\}_{i=1}^M$; that is, for some c in \mathbb{R}^M

$$\beta_* = \Sigma_{\beta} U c. \tag{E.16}$$

Our constraints in Eq. (E.15) then demand that $\langle \Sigma_{\beta} U[:,i], \Sigma_{\beta} U c \rangle = U[:,i]^{\top} \beta$ for each i, or equivalently that $U^{\top} \Sigma_{\beta} \Sigma_{\beta}^{-1} \Sigma_{\beta} U c = U^{\top} \beta$. This implies that $c = (U^{\top} \Sigma_{\beta} U)^{-1} U^{\top} \beta$. Plugging this into Eq. (E.16) yields $\beta_* = \Sigma_{\beta} U (U^{\top} \Sigma_{\beta} U)^{-1} U^{\top} \beta$, as desired.

E.5. Proof of Corollary 4.3

Recall that we wish to show that, for conjugate Bayesian regression, under \tilde{p} the uncertainty (i.e., posterior variance) for any linear combination of parameters, $\operatorname{Var}_{\tilde{p}}[v^{\top}\beta]$, is no smaller than the exact posterior variance. First, we note that this statement is formally equivalent to stating that $v^{\top}\tilde{\Sigma}_N v \geq v^{\top}\Sigma_N v$, or that $E:=\tilde{\Sigma}_N-\Sigma_N\succeq 0$ (where \succeq denotes positive definiteness). By Theorem 4.1, $\Sigma_N^{-1}-\tilde{\Sigma}_N^{-1}=\bar{U}\operatorname{diag}(\bar{\lambda}^2)\bar{U}^{\top}\succeq 0$. Since this implies that the inverse of the difference of these matrices is positive definite, we can then see that $(\Sigma_N^{-1}-\tilde{\Sigma}_N^{-1})^{-1}=\tilde{\Sigma}_N(\tilde{\Sigma}_N-\Sigma_N)^{-1}\Sigma_N\succeq 0$. Because, as valid covariance matrices, Σ_N and $\tilde{\Sigma}_N$ are both positive definite, and because inverses and product of positive definite matrices are positive definite, this implies that $\tilde{\Sigma}_N^{-1}\tilde{\Sigma}_N(\tilde{\Sigma}_N-\Sigma_N)^{-1}\Sigma_N\Sigma_N^{-1}=(\tilde{\Sigma}_N-\Sigma_N)^{-1}\succeq 0$. Finally, this implies that $\tilde{\Sigma}_N-\Sigma_N\succeq 0$ as desired.

E.6. Information loss due the LR-GLM approximation

We see similar behavior to that demonstrated in Corollary 4.3 in the following corollary, which shows that our approximate posterior never has lower entropy than the exact posterior. Concretely, we look at the reduction of entropy in the approximate posterior relative to the exact posterior (MacKay, 2003), where entropy is defined as:

$$H[p(\beta)] := \mathbb{E}_p[-\log_2 p(\beta)]$$

Corollary E.1. The entropy $H\left[\tilde{p}(\beta|X,Y)\right]$ is no less than $H\left[p(\beta|X,Y)\right]$. Furthermore, when using an isotropic Gaussian prior $\Sigma_{\beta} = \sigma_{\beta}^2 I$, the information loss relative to the exact posterior (in nats) is upper bounded as $H\left[\tilde{p}(\beta|X,Y)\right] - H\left[p(\beta|X,Y)\right] \leq \frac{\tau \sigma_{\beta}^2}{2} \sum_{i=1}^{D-M} \bar{\lambda}_i^2$.

This result formalizes the intuition that the LR-GLM approximation reduces the information about the parameter that we are able to extract from the data. Additionally, the upper bound tells us that when U is obtained via an M truncated SVD, at most $\tau \sigma_{\beta}^2 \bar{\lambda}_1^2/2$ additional nats of information would have been provided by using the M+1-truncated SVD.

Proof. The entropy of the exact and approximate posteriors are given as:

$$H(p) = -\frac{1}{2}\log|2\pi e \Sigma_N^{-1}| = -\frac{1}{2}\left[D\log 2\pi e + \sum_{i=1}^D \log(\sigma_\beta^{-2} + \tau \lambda_i^2)\right]$$

and

$$H(\tilde{p}) = -\frac{1}{2}\log|2\pi e\tilde{\Sigma}_N^{-1}| = -\frac{1}{2}\left[D\log 2\pi e + \sum_{i=1}^M \log(\sigma_\beta^{-2} + \tau\lambda_i^2) - \sum_{i=M+1}^D \log\sigma_\beta^{-2}\right].$$

Therefore, we conclude that

$$\begin{split} H\big[\tilde{p}(\beta|X)\big] - H\big[p(\beta|X)\big] &= -\frac{1}{2} \sum_{i=1}^{D-M} \log \sigma_{\beta}^{-2} + \frac{1}{2} \sum_{i=1}^{D-M} \log (\sigma_{\beta}^{-2} + \tau \bar{\lambda}_{i}^{2}) \\ &= \frac{1}{2} \sum_{i=1}^{D-M} \log \frac{\sigma_{\beta}^{-2} + \tau \bar{\lambda}_{i}^{2}}{\sigma_{\beta}^{-2}} \\ &= \frac{1}{2} \sum_{i=1}^{D-M} \log (1 + \frac{\tau}{\sigma_{\beta}^{-2}} \bar{\lambda}_{i}^{2}) \\ &\leq \frac{1}{2} \sum_{i=1}^{D-M} \frac{\tau}{\sigma_{\beta}^{-2}} \bar{\lambda}_{i}^{2} = \frac{\tau \sigma_{\beta}^{2}}{2} \sum_{i=1}^{D-M} \bar{\lambda}_{i}^{2}. \end{split}$$

That $H\big[\tilde{p}(\beta|X)\big] - H\big[p(\beta|X)\big] > 0$ follows from the monotonicity of \log , that $\log(1) = 0$, and that $\tau\sigma_{\beta}^2\bar{\lambda}_i^2 > 0$ for $i=1,\ldots,D-M$.

F. Proofs and further results for LR-Laplace in non-conjugate models

In the main text we introduced LR-Laplace as a method which takes advantage of low-rank approximations to provide computational gains when computing a Laplace approximation to the Bayesian posterior. In what follows we verify the theoretical justifications for this approach. Appendix F.1 provides a derivation of Algorithm 1 and demonstrates the time complexities of each step, serving as a proof of Theorem 5.1. The remainder of the section is devoted to the proofs and discussion of the theoretical properties of LR-Laplace.

F.1. Proof of Theorem 5.1

Proof of Theorem 5.1. The LR-Laplace approximation is defined by mean and covariance parameters, $\hat{\mu}$ and $\hat{\Sigma}$. We prove Theorem 5.1 in two parts. First, we show that $\hat{\mu}$ and $\hat{\Sigma}$ do in fact define the Laplace approximation of $\tilde{p}(\beta|X,Y)$, i.e. the

construction of $\hat{\mu}$ in Line 9 satisfies $\hat{\mu} = \arg \max_{\beta} \tilde{p}(\beta|X,Y)$ and that $\hat{\Sigma} = \left(-\nabla_{\beta}^2 \log \tilde{p}(\beta|X,Y)|_{\beta=\hat{\mu}}\right)^{-1}$. Second, we show that each step of Algorithm 1 may be computed in O(NDM) time with O(DM + NM) storage.

Correctness of $\hat{\mu}$ and $\hat{\Sigma}$

In Line 8, the definition of γ_* implies that $\gamma_* = \arg \max_{\gamma \in \mathbb{R}^M} \tilde{p}_{U^\top \beta | X, Y}(\gamma | X, Y)$ since

$$\begin{split} \log \tilde{p}_{U^\top \beta|X,Y}(\gamma|X,Y) &= \log \tilde{p}_{U^\top \beta}(\gamma) + \log \tilde{p}_{Y|X,U^\top \beta}(Y|X,\gamma) + C \\ &= \log p_{U^\top \beta}(\gamma) + \log p_{Y|X,\beta}(Y|X,U\gamma) + C \\ &= \log \mathcal{N}(\gamma|U^\top \mu_\beta, U^\top \Sigma_\beta U) + \sum_{i=1}^N \log p_{y|x,\beta}(y_i|x_i,U\gamma) + C \\ &= -\frac{1}{2}\gamma^\top U^\top \Sigma_\beta U\gamma + \sum_{i=1}^N \phi(y_i,x_i^\top U\gamma) + C', \end{split}$$

where line 1 uses Bayes' rule, line 2 uses the definition of \tilde{p} in Eq. (1), line 3 uses the normality the prior, and the assumed conditional independence of the responses given β , and line 4 follows from the definition of $\phi(\cdot, \cdot)$ and the assumption that $\mu_{\beta} = 0$. C and C' are constants which do not depend on γ . This together with the following result (proved in Appendix F.2) implies that as defined in Line 9 of Algorithm 1, $\hat{\mu} = \arg \max_{\beta} \tilde{p}(\beta|X,Y)$.

Lemma F.1. Suppose a Gaussian prior $p(\beta) = \mathcal{N}(\mu_{\beta}, \Sigma_{\beta})$, and let $\gamma_* := \arg \max_{\gamma \in \mathbb{R}^M} \log \tilde{p}_{U^{\top}\beta|X,Y}(\gamma|X,Y)$. Then $\hat{\mu} := \arg \max_{\beta \in \mathbb{R}^D} \log \tilde{p}(\beta|X,Y)$ may be written as $\hat{\mu} = U\gamma_* + \bar{U}\bar{U}^{\top}\Sigma_{\beta}U(U^{\top}\Sigma_{\beta}U)^{-1}\gamma_*$.

We now show that as defined in Line 12 of Algorithm 1, $\hat{\Sigma}$ is inverse of the Hessian of the negative log posterior, H. We see this by writing

$$\begin{split} H :&= \nabla_{\beta}^2 - \log \tilde{p}(\beta|X,Y)|_{\beta = \hat{\mu}} \\ &= \nabla_{\beta}^2 - \log \mathcal{N}(\beta|\mu_{\beta}, \Sigma_{\beta})|_{\beta = \hat{\mu}} + \nabla_{\beta}^2 \sum_{i=1}^N -\phi(y_i, x_i^\top U U^\top \beta)|_{\beta = \hat{\mu}} \\ &= \Sigma_{\beta}^{-1} + \sum_{i=1}^N -\phi''(y_i, x_i^\top U U^\top \hat{\mu}) x_i U U^\top x_i^\top \\ &= \Sigma_{\beta}^{-1} + U U^\top X^\top \operatorname{diag} \left(-\vec{\phi}''(Y, X U U^\top \hat{\mu}) \right) X U U^\top, \end{split}$$

where $\vec{\phi}''$ is the second derivative of ϕ . The Woodbury matrix lemma then provides that we may compute $\hat{\Sigma}_N := H^{-1}$ as

$$\hat{\Sigma}_N = \Sigma_\beta - \Sigma_\beta U \left(U^\top \Sigma_\beta U - \left\{ U^\top X^\top \operatorname{diag} \left[\vec{\phi}''(Y, XUU^\top \hat{\mu}) \right] XU \right\}^{-1} \right)^{-1} U^\top \Sigma_\beta,$$

which we have written as $\hat{\Sigma} := \Sigma_{\beta} - \Sigma_{\beta} UWU^{\top}\Sigma_{\beta}$ in Line 12 with $W^{-1} = U^{\top}\Sigma_{\beta}U - \left\{U^{\top}X^{\top}\operatorname{diag}\left[\vec{\phi}''(Y,XUU^{\top}\hat{\mu})\right]XU\right\}^{-1}$.

Time complexity of Algorithm 1

We now prove the asserted time and memory complexities for each line of Algorithm 1.

Algorithm 1 begins with the computation of the M-truncated SVD of $X^{\top} \approx U \operatorname{diag}(\lambda) V$. As discussed in Section 4.1, U may be found in $O(ND \log M)$ time. At the end of this step we must store the projected data $XU \in \mathbb{R}^{N,M}$ and the left singular vectors, $U \in \mathbb{R}^{D,M}$. Which demands O(NM + DM) memory, and the matrix multiply for XU requires O(NDM) time and is the bottleneck step of the algorithm. The matrix V need not be explicitly computed or stored.

The next stage of the algorithm is solving for $\hat{\mu} = \arg\max_{\beta} \log \tilde{p}(\beta|X,Y)$. This is done in two stages: in Line 8 find $\gamma_* = \arg\max_{\gamma \in \mathbb{R}^M} \log \tilde{p}_{U^\top \beta|X,Y}(\gamma|X,Y)$ as the solution to a convex optimization problem, and in Line 9 find $\hat{\mu}$ as $\hat{\mu} = U\gamma_* + \bar{U}\bar{U}^\top \Sigma_{\beta} U(U^\top \Sigma_{\beta} U)^{-1}\gamma_*$. Beginning with Line 8, we note that the function $\log \tilde{p}(U^\top \beta|X,Y) = 0$

 $\log p(\beta) + \log \tilde{p}(Y|X,\beta) + c \stackrel{c}{=} \log \mathcal{N}(U^\top \beta | U^\top \mu_\beta, U^\top \Sigma_\beta U) + \sum_{i=1}^N \log p(y_i | x_i^\top U U^\top \beta)$ is a finite sum of functions concave in β and therefore also in $U^\top \beta$. γ_* may therefore be solved to a fixed precision in O(NM) time under the assumptions of our theorem using stochastic optimization algorithms such as stochastic average gradient (Schmidt et al., 2017). In our experiments we use more standard batch convex optimization algorithm (L-BFGS-B (Zhu et al., 1997)) which takes at most $O(N^2M)$ time. This latter upper bound on complexity may be seen from observing each gradient evaluation takes O(NM) time (the cost for the likelihood evaluation, since computing the log prior and its gradient is $O(M^2)$ after computing $U^\top \Sigma_\beta U$ once, which takes $O(DM^2)$ time by assumption) and the number of iterations required can grow up to linearly in the maximum eigenvalue of Hessian, which in turn grows linearly in N (Boyd & Vandenberghe, 2004).

The second step is computing $\hat{\mu} = U\gamma_* + \bar{U}\bar{U}^{\top}\Sigma_{\beta}U(U^{\top}\Sigma_{\beta}U)^{-1}\gamma_*$. Given γ_* , this may be computed in O(DM) time, which one may see by noting that $\bar{U}\bar{U}^{\top}$ (which we never explicitly compute) may be written as $\bar{U}\bar{U}^{\top} = (I - UU^{\top})$, and finding $\hat{\mu}$ as $\hat{\mu} = U\gamma_* + \Sigma_{\beta}U(U^{\top}\Sigma_{\beta}U)^{-1}\gamma_* - UU^{\top}\Sigma_{\beta}U(U^{\top}\Sigma_{\beta}U)^{-1}\gamma_*$. By assumption, the structure of Σ_{β} allows us to compute $U^{\top}\Sigma_{\beta}U$ in $O(DM^2)$ time and matrix vector products with Σ_{β} in O(D) time.

We now turn to the third stage of the algorithm, solving for the posterior covariance $\hat{\Sigma}$, which is represented as an expression of U, Σ_{β} and W, defined in Line 11. Computing W requires O(DM) and $O(NM^2)$ matrix multiplications (since we have precomputed XU), and two $O(M^3)$ matrix inversions which comes to $O(NM^2 + DM)$ time. The memory complexity of this step is O(NM) since it involves handling XU. Once W has been computed we may use the representation $\hat{\Sigma} = \Sigma_{\beta} - \Sigma_{\beta} UWU^{\top} \Sigma_{\beta}$ as presented in Line 12. This representation does not entail performing any additional computation (which is why we have written O(0)), but as this expression includes U, storing $\hat{\Sigma}$ requires O(DM) memory.

Lastly, we may immediately see that computing posterior variances and covariances takes only $O(M^2)$ time as it involves only indexing into Σ_{β} and U and $O(M^2)$ matrix-vector multiplies.

F.2. Proof of Lemma F.1

We prove the lemma by constructing a rotation of the parameter space by the matrix of singular vectors $[U, \bar{U}]$, in which we have the prior

$$p\bigg(\begin{bmatrix} U^{\top}\beta \\ \bar{U}^{\top}\beta \end{bmatrix}\bigg) = \mathcal{N}\bigg(\begin{bmatrix} U^{\top}\beta \\ \bar{U}^{\top}\beta \end{bmatrix} \middle| \begin{bmatrix} U^{\top}\mu_{\beta} \\ \bar{U}^{\top}\mu_{\beta} \end{bmatrix}, \begin{bmatrix} U^{\top}\Sigma_{\beta}U, \ U^{\top}\Sigma_{\beta}\bar{U} \\ \bar{U}^{\top}\Sigma_{\beta}U, \ \bar{U}^{\top}\Sigma_{\beta}\bar{U} \end{bmatrix}\bigg).$$

We have that

$$\begin{split} \hat{\mu} &:= \underset{\beta \in \mathbb{R}^{D}}{\arg \max} \log \tilde{p}(\beta|X,Y) \\ &= \left[U \, \bar{U} \right] \underset{U^{\top}\beta \in \mathbb{R}^{M}, \bar{U}^{\top}\beta \in \mathbb{R}^{D-M}}{\arg \max} \log \tilde{p}\left(\left[\begin{matrix} U^{\top}\beta \\ \bar{U}^{\top}\beta \end{matrix} \right] | X,Y \right) \\ &= U \underset{U^{\top}\beta \in \mathbb{R}^{M}}{\arg \max} \left(\log \tilde{p}(U^{\top}\beta|X,Y) + \bar{U} \underset{\bar{U}^{\top}\beta \in \mathbb{R}^{D-M}}{\arg \max} \log \tilde{p}(\bar{U}^{\top}\beta|U^{\top}\beta,X,Y) \right) \\ &= U \underset{U^{\top}\beta \in \mathbb{R}^{M}}{\arg \max} \log \tilde{p}(U^{\top}\beta|X,Y) + \\ \bar{U} \underset{\bar{U}^{\top}\beta \in \mathbb{R}^{M}}{\arg \max} \log \mathcal{N}(\bar{U}^{\top}\beta|\bar{U}^{\top}\Sigma_{\beta}U(U^{\top}\Sigma_{\beta}U)^{-1}U^{\top}\beta, \bar{U}\Sigma_{\beta}\bar{U} - \bar{U}\Sigma_{\beta}U(U^{\top}\Sigma_{\beta}U)U^{\top}\Sigma_{\beta}\bar{U} \right) \\ &= U\gamma_{*} + \bar{U}\bar{U}^{\top}\Sigma_{\beta}U(U^{\top}\Sigma_{\beta}U)^{-1}\gamma_{*}. \end{split}$$

In the second line we simply move to the rotated parameter space. In the third line, we use the chain rule of probability to separate out two terms. To produce the fourth line, we note that since $\tilde{p}(Y|X,\beta) = p(Y|XUU^{\top}\beta) = \tilde{p}(Y|X,U^{\top}\beta)$, that Y and $\bar{U}^{\top}\beta$ are conditionally independent given $U^{\top}\beta$. We next note that though $\arg\max_{\bar{U}^{\top}\beta\in\mathbb{R}^{D-M}}\log p(\bar{U}^{\top}\beta|U^{\top}\beta)$ depends on $U^{\top}\beta$, $\max_{\bar{U}^{\top}\beta\in\mathbb{R}^{D-M}}\log p(\bar{U}^{\top}\beta|U^{\top}\beta)$ does not depend $U^{\top}\beta$. This allows us to use the definition of γ_* to arrive at the fifth line, as desired.

In the special case that Σ_{β} is diagonal, this expression reduces to $U\gamma_*$. This can be seen by recognizing that $\bar{U}^{\top}\Sigma_{\beta}U$ is then diag(0).

F.3. Proof of Theorem 5.2

Our approach to proving Theorem 5.2 follows a similar approach to that taken to prove Theorem 4.1. In particular, we begin by upper bounding the norm of the error of the gradients at the approximate MAP. Noting that the strong log concavity of the exact posterior, which having been assumed to hold globally, must then also hold on $\{t\hat{\mu} + (1-t)\bar{\mu}|t\in[0,1]\}$, we obtain an upper-bound on $\|\hat{\mu} - \bar{\mu}\|_2$ by again applying Lemma E.1.

To begin, we first recall that the exact and LR-GLM posteriors may be written as

$$\log p(\beta|X, Y) = \log p(\beta) + \sum_{n=1}^{N} \phi(y_n|x_n^{\top}\beta) - \log Z$$

and

$$\log \tilde{p}(\beta|X,Y) = \log p(\beta) + \sum_{n=1}^{N} \phi(y_n, x_n^{\top} U U^{\top} \beta) - \log \tilde{Z}$$

where $\phi(\cdot,\cdot)$ is such that $\phi(y,a) = \log p(y|x^{\top}\beta = a)$, and Z and \tilde{Z} are the normalizing constants of the exact and approximate posteriors. As a result, the gradients of these log densities are given as

$$\nabla_{\beta} \log p(\beta|X,Y) = \nabla_{\beta} \log p(\beta) + X^{\top} \vec{\phi}'(Y,X\beta)$$

and

$$\nabla_{\beta} \log \tilde{p}(\beta | X, Y) = \nabla_{\beta} \log p(\beta) + UU^{\top} X^{\top} \vec{\phi}'(Y, XUU^{\top} \beta),$$

where $\vec{\phi}'(Y, X\beta) \in \mathbb{R}^N$ is such that for each $n \in [N]$, $\vec{\phi}'(Y, X\beta)_n = \frac{d}{da}\phi(y_n, a)|_{a=x_n^\top\beta}$.

And the difference in the gradients is

$$\nabla_{\beta} \log p(\beta | X, Y) - \nabla_{\beta} \log \tilde{p}(\beta | X, Y) = X^{\top} \vec{\phi}'(Y, X\beta) - UU^{\top} X^{\top} \vec{\phi}'(Y, XUU^{\top}\beta). \tag{F.1}$$

Appealing to Taylor's theorem, we may write for any β that

$$\phi'(y_n, x_n^\top U U^\top \beta) = \phi'(y_n, x_n^\top \beta) + (x_n^\top U U^\top \beta - x_n^\top \beta) \phi''(y_n, a_n)$$

for some $a_n \in [x_n^\top U U^\top \beta, x_n^\top \beta]$, where $\phi''(y, a) := \frac{d^2}{da^2} \phi(y, a)$.

Using this and introducing vectorized notation for ϕ'' to match that used for $\vec{\phi}'$, we may rewrite the difference in the gradients as

$$\nabla_{\beta} \log p(\beta|X,Y) - \nabla_{\beta} \log \tilde{p}(\beta|X,Y)$$

$$= X^{\top} \vec{\phi}'(Y,X\beta) - UU^{\top} X^{\top} \vec{\phi}'(Y,X\beta) - UU^{\top} X^{\top} [(XUU^{\top}\beta - X^{\top}\beta) \circ \vec{\phi}''(Y,A)]$$

$$= \bar{U}\bar{U}^{\top} X^{\top} \vec{\phi}'(Y,X\beta) + UU^{\top} X^{\top} [(X\bar{U}\bar{U}^{\top}\beta) \circ \vec{\phi}''(Y,A)],$$

where $A \in \mathbb{R}^N$ is such that for each $n \in [N]$, $A_n \in [x_n^\top U U^\top \beta, x_n^\top \beta]$, and \circ denotes element-wise scalar multiplication.

We can use this to derive an upper bound on the norm of the difference of the gradients as

$$\|\nabla_{\beta} \log p(\beta|X,Y) - \nabla_{\beta} \log \tilde{p}(\beta|X,Y)\|_{2} = \|\bar{U}\bar{U}^{\top}X^{\top}\vec{\phi}' + UU^{\top}X^{\top}[(X\bar{U}\bar{U}^{\top}\beta) \circ \vec{\phi}'']\|_{2}$$

$$\leq \|\bar{U}\bar{U}^{\top}X^{\top}\vec{\phi}'\|_{2} + \|UU^{\top}X^{\top}[(X\bar{U}\bar{U}^{\top}\beta) \circ \vec{\phi}'']\|_{2}$$

$$\leq \bar{\lambda}_{1}\|\vec{\phi}'\|_{2} + \lambda_{1}\|(X\bar{U}\bar{U}^{\top}\beta) \circ \vec{\phi}''\|_{2}$$

$$\leq \bar{\lambda}_{1}\|\vec{\phi}'\|_{2} + \lambda_{1}\bar{\lambda}_{1}\|\bar{U}^{\top}\beta\|_{2}\|\vec{\phi}''\|_{\infty}$$

$$= \bar{\lambda}_{1}(\|\vec{\phi}'\|_{2} + \lambda_{1}\|\bar{U}^{\top}\beta\|_{2}\|\vec{\phi}''\|_{\infty}),$$

where we have written $\vec{\phi}'$ and $\vec{\phi}''$ in place of $\vec{\phi}'(Y, X\beta)$ and $\vec{\phi}''(Y, A)$, respectively, for brevity despite their dependence on β .

Next, let α be the strong log-concavity parameter of $p(\beta|X,Y)$. Lemma E.1 then implies that

$$\|\hat{\mu} - \bar{\mu}\|_{2} \leq \frac{\bar{\lambda}_{1}(\|\vec{\phi}'(Y, X\hat{\mu})\|_{2} + \lambda_{1}\|\bar{U}^{\top}\hat{\mu}\|_{2}\|\vec{\phi}''(Y, A)\|_{\infty})}{\alpha}$$

as desired, where for each $n \in [N]$, $A_n \in [x_n^\top U U^\top \hat{\mu}, x_n^\top \hat{\mu}]$.

F.4. Bounds on derivatives of higher order for the log-likelihood in logistic regression and other GLMs

We here provide some additional support for the claim that in Remark 5.3 that the higher order derivatives of the log-likelihood function, ϕ , are well-behaved. For logistic regression (which we explore in detail below), for any y in $\{-1,1\}$ and a in \mathbb{R} , it holds that $|\frac{\partial}{\partial a}\phi(y,a)| \leq 1$ and $|\frac{\partial^2}{\partial^2 a}\phi(y,a)| \leq \frac{1}{4}$. For Poisson regression with $\phi(y,a) = \log \operatorname{Pois}(y|\lambda = \log(1+\exp\{a\}))$, both $|\frac{\partial}{\partial a}(y,a)|$ and $|\frac{\partial^2}{\partial^2 a}\phi(y,a)|$ are bounded by a small constant factor of y. Additionally, in these cases $|\frac{\partial^3}{\partial a^3}\phi(y,a)|$ is also well behaved, a fact relevant to Corollary 5.6. However, for alternative mapping functions for Poisson regression, e.g. defining $\mathbb{E}[y_i|x_i,\beta] = \exp\{x_i^{\top}\beta\}$, these derivatives will grow exponentially quickly with $x_i^{\top}\beta$, which illustrates that our provided bounds are sensitive to the particular form chosen for the GLM likelihood.

We now move to compute explicit upper bounds on the derivatives of the log likelihood in logistic regression. This produces the constants mentioned above, and permits easy computation of upper bounds on the bounds on the approximation error of LR-Laplace provided in Theorem 5.2 and Corollary 5.6. In particular the logistic regression mapping function (Huggins et al., 2017) is given as

$$\phi(y_n, x_n^\top \beta) = -\log\left(1 + \exp\{-y_n x_n^\top \beta\}\right),\tag{F.2}$$

where each $y_n \in \{-1, 1\}$.

The first three derivatives of this mapping function and bounds on their absolute values are as follows:

$$\phi'(y_n, x_n^{\top}\beta) := \frac{d}{da}\phi(y_n, a)\big|_{a = x_n^{\top}\beta} = y_n \frac{\exp\{-yx_n^{\top}\beta\}}{1 + \exp\{-y_nx_n^{\top}\beta\}}$$
(F.3)

Notably, $\forall a \in \mathbb{R}, y \in \{-1, 1\}, |\phi'(y, a)| < 1$ and

$$\phi''(y_n, x_n^{\top} \beta) := \frac{d^2}{da^2} \phi(y, a) \Big|_{a = x_n^{\top} \beta} = -(1 + \exp\{x_n^{\top} \beta\})^{-1} (1 + \exp\{-x_n^{\top} \beta\})^{-1}.$$
 (F.4)

Furthermore, for any a in \mathbb{R} and y in $\{-1,1\}$, $-\frac{1}{4} \le \phi''(y,a) < 0$. This implies that the Hessian of the negative log likelihood will be positive semi-definite everywhere. We additionally have

$$\frac{d^3}{da^3}\phi(y,a) = \phi'''(a) = \frac{\left(\exp\{a\}(\exp(-a) - 1)\right)}{(1 + \exp\{a\})^3}$$
(F.5)

which for any a in \mathbb{R} satisfies, $-\frac{1}{6\sqrt{3}} \le \phi'''(a) \le \frac{1}{6\sqrt{3}}$.

F.5. Asymptotic inconsistency of the approximate posterior mean within the span of the projections

Consider a Bayesian logistic regression, in which

$$x_i \sim \mathcal{N}\Big(\begin{bmatrix}0\\0\end{bmatrix}, \begin{bmatrix}1&0\\0&0.99\end{bmatrix}\Big), \qquad \qquad \beta = \begin{bmatrix}10\\1000\end{bmatrix}, \qquad \qquad y_i \sim \mathrm{Bern}\Big((1 + \exp\{x_i^\top\beta\})^{-1}\Big).$$

In this setting, a rank 1 approximation of the design will capture only the first dimension of data (i.e. $U_N \to U_* = [1,0]$). However the second dimension explains almost all of the variance in the responses. As such $y_i|U_*^\top x_i$, $\beta \stackrel{d}{\approx} \operatorname{Bern}(1/2)$ and we will get $U_*^\top \beta |X,Y=\beta_1|X,Y\approx 0.0$ under \tilde{p} .

F.6. Proof of Corollary 5.6

Our proof proceeds via an upper bound on the $(2, \hat{p})$ -Fisher distance between \hat{p} and \bar{p} (Huggins et al., 2018). Specifically, the $(2, \hat{p})$ -Fisher distance given by

$$d_{2,\hat{p}}(\hat{p},\bar{p}) = \left(\int \|\nabla_{\beta} \log \hat{p}(\beta) - \nabla_{\beta} \log \bar{p}(\beta)\|_{2}^{2} dp(\beta)\right)^{\frac{1}{2}}.$$
 (F.6)

Given the strong log-concavity of \bar{p} , our upper bound on this Fisher distance immediately provides an upper-bound on the 2-Wasserstein distance (Huggins et al., 2018).

We first recall that \hat{p} and \bar{p} are defined by Laplace approximations of $\tilde{p}(\beta|X,Y)$ and $p(\beta|X,Y)$ respectively. As such we have that

$$\log \hat{p}(\beta) \stackrel{c}{=} -\frac{1}{2}(\beta - \hat{\mu})^{\top} \left(\Sigma_{\beta}^{-1} - UU^{\top}X^{\top} \operatorname{diag}(\vec{\phi}''(Y, XUU^{\top}\hat{\mu}))XUU^{\top}\right)(\beta - \hat{\mu})$$

where $\vec{\phi}''(Y, XUU^{\top}\hat{\mu})$ is defined as in Algorithm 1 such that $\vec{\phi}''(Y, X\beta)_i = \frac{d^2}{da^2} \log p(y_i|x^{\top}\beta = a)|_{a=x_i^{\top}\beta}$, and

$$\log \bar{p}(\beta) \stackrel{c}{=} -\frac{1}{2} (\beta - \bar{\mu})^{\top} (\Sigma_{\beta}^{-1} - X^{\top} \operatorname{diag}(\vec{\phi}''(Y, X\bar{\mu})) X) (\beta - \bar{\mu}).$$

Accordingly,

$$\nabla_{\beta} \log \hat{p}(\beta) = -(\beta - \hat{\mu})^{\top} \left(\Sigma_{\beta}^{-1} - UU^{\top} X^{\top} \operatorname{diag}(\vec{\phi}''(Y, XUU^{\top} \hat{\mu})) XUU^{\top} \right)$$

and

$$\nabla_{\beta} \log \bar{p}(\beta) = -(\beta - \bar{\mu})^{\top} \left[\Sigma_{\beta}^{-1} - X^{\top} \operatorname{diag}(\vec{\phi}''(Y, X\bar{\mu})) X \right]$$

To define an upper bound on $d_{2,\hat{p}}(\hat{p},p)$, we must consider the difference between the gradients,

$$\begin{split} \nabla_{\beta} \log \hat{p}(\beta) - \nabla_{\beta} \log \bar{p}(\beta) &= -(\beta - \hat{\mu})^{\top} \left\{ \Sigma_{\beta}^{-1} - UU^{\top} X^{\top} \mathrm{diag}[\vec{\phi}''(Y, XUU^{\top} \hat{\mu})] X U U^{\top} \right\} \\ &+ (\beta - \bar{\mu})^{\top} \left\{ \Sigma_{\beta}^{-1} - X^{\top} \mathrm{diag}[\vec{\phi}''(Y, X\bar{\mu})] X \right\} \\ &= (\hat{\mu} - \bar{\mu}) \Sigma_{\beta}^{-1} + (\beta - \hat{\mu})^{\top} U U^{\top} X^{\top} \mathrm{diag}[\vec{\phi}''(Y, XUU^{\top} \hat{\mu})] X U U^{\top} \\ &- (\beta - \bar{\mu})^{\top} X^{\top} \mathrm{diag}[\vec{\phi}''(Y, X\bar{\mu})] X. \end{split}$$

Appealing to Taylor's theorem, we can rewrite $\vec{\phi}''(Y, XUU^{\top}\hat{\mu})$ as

$$\begin{split} \vec{\phi}''(Y, XUU^{\top}\hat{\mu}) &= \vec{\phi}''(Y, X\bar{\mu}) + (XUU^{\top}\hat{\mu} - X\bar{\mu}) \circ \vec{\phi}'''(Y, A) \\ &= \vec{\phi}''(Y, X\bar{\mu}) + (XUU^{\top}\hat{\mu} - X\hat{\mu} + X(\hat{\mu} - \bar{\mu})) \circ \vec{\phi}'''(Y, A) \\ &= \vec{\phi}''(Y, X\bar{\mu}) - X\bar{U}\bar{U}^{\top} \circ \vec{\phi}'''(Y, A) + X(\hat{\mu} - \bar{\mu}) \circ \vec{\phi}'''(Y, A) \\ &= \vec{\phi}''(Y, X\bar{\mu}) + R, \end{split}$$

where the first line follows from Taylor's theorem by appropriately choosing each $A_i \in [x_i^\top U U^\top \hat{\mu}, x_i^\top \bar{\mu}]$, and in the fourth line we substitute in $R := -X \bar{U} \bar{U}^\top \circ \vec{\phi}'''(Y, A) + X(\hat{\mu} - \bar{\mu}) \circ \vec{\phi}'''(Y, A)$.

We now can rewrite the difference in the gradients as

$$\begin{split} \nabla_{\beta} \log \hat{p}(\beta) - \nabla_{\beta} \log \bar{p}(\beta) &= (\hat{\mu} - \bar{\mu}) \Sigma_{\beta}^{-1} \\ &+ (\beta - \hat{\mu})^{\top} U U^{\top} X^{\top} \mathrm{diag}[\vec{\phi}''(Y, X \bar{\mu})] X U U^{\top} \\ &+ (\beta - \hat{\mu})^{\top} U U^{\top} X^{\top} \mathrm{diag}(R) X U U^{\top} \\ &- (\beta - \bar{\mu})^{\top} X^{\top} \mathrm{diag}(\vec{\phi}''(Y, X \bar{\mu})) X \\ &= (\hat{\mu} - \bar{\mu})^{\top} (\Sigma_{\beta}^{-1} - U U^{\top} X^{\top} \mathrm{diag}[\vec{\phi}''(Y, X \bar{\mu})] X U U^{\top}) \\ &+ (\beta - \hat{\mu})^{\top} U U^{\top} X^{\top} \mathrm{diag}(R) X U U^{\top} \\ &- (\beta - \bar{\mu})^{\top} \bar{U} \bar{U}^{\top} X^{\top} \mathrm{diag}(\vec{\phi}''(Y, X \bar{\mu})) X \bar{U} \bar{U}^{\top} \\ &- (\beta - \bar{\mu})^{\top} \bar{U} \bar{U}^{\top} X^{\top} \mathrm{diag}(\vec{\phi}''(Y, X \bar{\mu})) X U U^{\top} \\ &- (\beta - \bar{\mu})^{\top} \bar{U} \bar{U}^{\top} X^{\top} \mathrm{diag}(\vec{\phi}''(Y, X \bar{\mu})) X \bar{U} \bar{U}^{\top}. \end{split}$$

Which is obtained by first writing $X^{\top} \mathrm{diag}[\vec{\phi}''(Y, X\bar{\mu})]X$ in the fourth line as $(UU^{\top}X^{\top} + \bar{U}\bar{U}^{\top}X^{\top})\mathrm{diag}[\vec{\phi}''(Y, X\bar{\mu})](XUU^{\top} + X\bar{U}\bar{U}^{\top})$, multiplying through and rearranging the resulting terms.

Given this form of the difference in the gradients, we may upper bound its norm as

$$\begin{split} \|\nabla_{\beta} \log \hat{p}(\beta) - \nabla_{\beta} \log \bar{p}(\beta)\|_{2} &\leq \|\hat{\mu} - \bar{\mu}\|_{2} \|\Sigma_{\beta}^{-1} - UU^{\top}X^{\top} \mathrm{diag}[\vec{\phi}''(Y, X\bar{\mu})] X U U^{\top}\|_{2} \\ &+ \|\beta - \hat{\mu}\|_{2} \|UU^{\top}X^{\top} \mathrm{diag}(R) X U U^{\top}\|_{2} \\ &+ \|\beta - \bar{\mu}\|_{2} \|UU^{\top}X^{\top} \mathrm{diag}[\vec{\phi}''(Y, X\bar{\mu})] X \bar{U} \bar{U}^{\top} + \\ &\bar{U}\bar{U}^{\top}X^{\top} \mathrm{diag}[\vec{\phi}''(Y, X\bar{\mu})] X U U^{\top} + \bar{U}\bar{U}^{\top}X^{\top} \mathrm{diag}[\vec{\phi}''(Y, X\bar{\mu})] X \bar{U}\bar{U}^{\top}\|_{2} \\ &\leq \|\hat{\mu} - \bar{\mu}\|_{2} \|\Sigma_{\beta}^{-1} - UU^{\top}X^{\top} \mathrm{diag}[\vec{\phi}''(Y, X\bar{\mu})] X U U^{\top}\|_{2} \\ &+ \|\beta - \hat{\mu}\|_{2} \|UU^{\top}X^{\top} \mathrm{diag}(R) X U U^{\top}\|_{2} \\ &+ \|\beta - \bar{\mu}\|_{2} \{\|\bar{U}\bar{U}^{\top}X^{\top} \mathrm{diag}[\vec{\phi}''(Y, X\bar{\mu})] X \bar{U}\bar{U}^{\top}\|_{2} + \\ &2 \|\bar{U}\bar{U}^{\top}X^{\top} \mathrm{diag}[\vec{\phi}''(Y, X\bar{\mu})] X U U^{\top}\|_{2} \} \end{split}$$

by the triangle inequality.

$$\leq \|\hat{\mu} - \bar{\mu}\|_{2} \left\{ \|\Sigma_{\beta}^{-1}\|_{2} + \|U \operatorname{diag}(\lambda) V^{\top}\|_{2} \|\operatorname{diag}[\vec{\phi}''(Y, X\bar{\mu})]\|_{2} \|V \operatorname{diag}(\lambda) U^{\top}\|_{2} \right\}$$

$$+ \|\beta - \hat{\mu}\|_{2} \|U \operatorname{diag}(\lambda) V^{\top}\|_{2} \|\operatorname{diag}(R)\|_{2} \|V \operatorname{diag}(\lambda) U^{\top}\|_{2}$$

$$+ \|\beta - \bar{\mu}\|_{2} \left\{ \|\bar{U} \operatorname{diag}(\bar{\lambda}) \bar{V}^{\top}\|_{2} \|\operatorname{diag}[\vec{\phi}''(Y, X\bar{\mu})]\|_{2} \|\bar{V} \operatorname{diag}(\bar{\lambda}) \bar{U}^{\top}\|_{2} +$$

$$2 \|\bar{U}^{\top} \operatorname{diag}(\bar{\lambda}) \bar{V}^{\top}\|_{2} \|\operatorname{diag}[\vec{\phi}''(Y, X\bar{\mu})]\|_{2} \|V \operatorname{diag}(\lambda) U^{\top}\|_{2} \right\}$$

by again using the triangle inequality, and decomposing X^{\top} into $U \operatorname{diag}(\lambda) V^{\top} + \bar{U} \operatorname{diag}(\bar{\lambda}) \bar{V}^{\top}$.

$$\leq \|\hat{\mu} - \bar{\mu}\|_2 \left(\|\Sigma_{\beta}^{-1}\|_2 + \lambda_1^2 \|\vec{\phi}''\|_{\infty} \right) + \lambda_1^2 \|\beta - \hat{\mu}\|_2 \|R\|_{\infty} + (\bar{\lambda}_1^2 + 2\lambda_1 \bar{\lambda}_1) \|\beta - \bar{\mu}\|_2 \|\vec{\phi}''\|_2,$$

where in the last line we have shortened $\vec{\phi}''(Y, X\bar{\mu})$ to $\vec{\phi}''$ for convenience.

Next noting that $\|\bar{\mu} - \hat{\mu}\|_2 \leq \bar{\lambda}_1 c$ for $c := \frac{\|\vec{\phi}'(Y, X\hat{\mu})\|_2 + \lambda_1 \|\bar{U}^\top \hat{\mu}\|_2 \|\vec{\phi}''(Y, A)\|_\infty}{\alpha}$, where α is the strong log concavity parameter of $p(\beta|X,Y)$ (which follows from Theorem 5.2), we can see that $\|R\|_\infty \leq \bar{\lambda}_1 r$ where $r := (\|U^\top \hat{\mu}\|_\infty \|\vec{\phi}'''(Y,A)\|_\infty + \lambda_1 c \|\vec{\phi}'''(Y,A)\|_\infty)$. That r is bounded follows from the assumption that $\log p(y|x,\beta)$ has bounded third derivatives, an equivalent to a Lipschitz condition on ϕ'' . We can next simplify this upper bound to

$$\begin{split} \|\nabla_{\beta}\log\hat{p}(\beta) - \nabla_{\beta}\log\bar{p}(\beta)\|_{2} &\leq \bar{\lambda}_{1}c[\|\Sigma_{\beta}^{-1}\|_{2} + \lambda_{1}^{2}\|\vec{\phi}''\|_{\infty}] + \lambda_{1}^{2}\bar{\lambda}_{1}r\|\beta - \hat{\mu}\|_{2} + \bar{\lambda}_{1}(\bar{\lambda}_{1} + 2\lambda_{1})\|\beta - \bar{\mu}\|_{2}\|\vec{\phi}''\|_{\infty} \\ &= \bar{\lambda}_{1}\left[c(\|\Sigma_{\beta}^{-1}\|_{2} + \lambda_{1}^{2}\|\vec{\phi}''\|_{\infty}) + \lambda_{1}^{2}r\|\beta - \hat{\mu}\|_{2} + (\bar{\lambda}_{1} + 2\lambda_{1})\|\beta - \bar{\mu}\|_{2}\|\vec{\phi}''\|_{\infty}\right] \\ &\leq \bar{\lambda}_{1}\left[c(\|\Sigma_{\beta}^{-1}\|_{2} + \lambda_{1}^{2}\|\vec{\phi}''\|_{\infty}) + \lambda_{1}^{2}r\|\beta - \hat{\mu}\|_{2} + (\bar{\lambda}_{1} + 2\lambda_{1})(\|\hat{\mu} - \bar{\mu}\|_{2} + \|\beta - \hat{\mu}\|_{2})\|\vec{\phi}''\|_{\infty}\right] \\ &\text{by the triangle inequality.} \end{split}$$

$$\leq \bar{\lambda}_{1} \left[c(\|\Sigma_{\beta}^{-1}\|_{2} + \lambda_{1}^{2}\|\vec{\phi}''\|_{\infty}) + \lambda_{1}^{2}r\|\beta - \hat{\mu}\|_{2} + (\bar{\lambda}_{1} + 2\lambda_{1})(\bar{\lambda}_{1}c + \|\beta - \hat{\mu}\|_{2})\|\vec{\phi}''\|_{\infty} \right]$$

$$= \bar{\lambda}_{1} \left[c(\|\Sigma_{\beta}^{-1}\|_{2} + \lambda_{1}^{2}\|\vec{\phi}''\|_{\infty}) + c(\bar{\lambda}_{1}^{2} + 2\lambda_{1}\bar{\lambda}_{1})\|\vec{\phi}''\|_{\infty} + (\lambda_{1}^{2}r + (\bar{\lambda}_{1} + 2\lambda_{1})\|\vec{\phi}''\|_{\infty})\|\beta - \hat{\mu}\|_{2} \right]$$

$$= \bar{\lambda}_{1} \left[c(\|\Sigma_{\beta}^{-1}\|_{2} + (\lambda_{1} + \bar{\lambda}_{1})^{2}\|\vec{\phi}''\|_{\infty}) + (\lambda_{1}^{2}r + (\bar{\lambda}_{1} + 2\lambda_{1})\|\vec{\phi}''\|_{\infty})\|\beta - \hat{\mu}\|_{2} \right].$$

Thus, taking the expectation of this upper bound on the norm squared over β with respect to \hat{p} we get

$$\begin{split} d_{2,\hat{p}}^2(\hat{p},p) &\leq \mathbb{E}_{\hat{p}(\beta)} \left(\bar{\lambda}_1^2 \left\{ c \left[\| \Sigma_{\beta}^{-1} \|_2 + (\lambda_1 + \bar{\lambda}_1)^2 \| \vec{\phi}'' \|_{\infty} \right] + \left[\lambda_1^2 r + (\bar{\lambda}_1 + 2\lambda_1) \| \vec{\phi}'' \|_{\infty} \right] \| \beta - \hat{\mu} \|_2 \right\}^2 \right) \\ &\leq 2 \bar{\lambda}_1^2 \mathbb{E}_{\hat{p}(\beta)} \left\{ c^2 \left[\| \Sigma_{\beta}^{-1} \|_2 + (\lambda_1 + \bar{\lambda}_1)^2 \| \vec{\phi}'' \|_{\infty} \right]^2 + \left[\lambda_1^2 r + (\bar{\lambda}_1 + 2\lambda_1) \| \vec{\phi}'' \|_{\infty} \right]^2 \| \beta - \hat{\mu} \|_2^2 \right\} \\ &\text{since } \forall a, b \in \mathbb{R}, (a + b)^2 \leq 2(a^2 + b^2) \\ &= 2 \bar{\lambda}_1^2 \left\{ c^2 \left[\| \Sigma_{\beta}^{-1} \|_2 + (\lambda_1 + \bar{\lambda}_1)^2 \| \vec{\phi}'' \|_{\infty} \right]^2 + \left[\lambda_1^2 r + (\bar{\lambda}_1 + 2\lambda_1) \| \vec{\phi}'' \|_{\infty} \right]^2 \mathbb{E}_{\hat{p}(\beta)} [\| \beta - \hat{\mu} \|_2^2] \right\} \\ &= 2 \bar{\lambda}_1^2 \left\{ c^2 \left[\| \Sigma_{\beta}^{-1} \|_2 + (\lambda_1 + \bar{\lambda}_1)^2 \| \vec{\phi}'' \|_{\infty} \right]^2 + \left[\lambda_1^2 r + (\bar{\lambda}_1 + 2\lambda_1) \| \vec{\phi}'' \|_{\infty} \right]^2 \operatorname{tr}(\hat{\Sigma}) \right\}. \end{split}$$

Next noting that \bar{p} is strongly $\|\bar{\Sigma}\|_2^{-1}$ log-concave, we may apply Theorem F.1, stated below, to obtain that

$$\begin{split} W_2(\hat{p},\bar{p}) &\leq \|\bar{\Sigma}\|_2 \sqrt{2\bar{\lambda}_1^2 \left\{ c^2 \left[\|\Sigma_{\beta}^{-1}\|_2 + (\lambda_1 + \bar{\lambda}_1)^2 \|\vec{\phi}''\|_{\infty} \right]^2 + \left[\lambda_1^2 r + (\bar{\lambda}_1 + 2\lambda_1) \|\vec{\phi}''\|_{\infty} \right]^2 \operatorname{tr}(\hat{\Sigma}) \right\}} \\ &\leq \sqrt{2}\bar{\lambda}_1 \|\bar{\Sigma}\|_2 \left\{ c \left[\|\Sigma_{\beta}^{-1}\|_2 + (\lambda_1 + \bar{\lambda}_1)^2 \|\vec{\phi}''\|_{\infty} \right] + \left[\lambda_1^2 r + (\bar{\lambda}_1 + 2\lambda_1) \|\vec{\phi}''\|_{\infty} \right] \sqrt{\operatorname{tr}(\hat{\Sigma})} \right\}, \end{split}$$

which is our desired upper bound.

Theorem F.1. Suppose that $p(\beta)$ and $q(\beta)$ are twice continuously differentiable and that q is α -strongly log concave. Then

$$W_2(p,q) \le \alpha^{-1} d_{2,p}(p,q),$$

where W_2 denotes the 2-Wasserstein distance between p and q.

Proof. This follows from Huggins et al. (2018) Theorem 5.2, or similarly from Bolley et al. (2012) Lemma 3.3 and Proposition 3.10. \Box

F.7. Proof of bounded asymptotic error

We here provide a formal statement and proof of Theorem 5.7, detailing the required regularity conditions.

Theorem F.2 (Asymptotic). Assume $x_i \overset{\text{i.i.d.}}{\sim} p_*$ for some distribution p_* such that $\mathbb{E}_{p_*}[x_ix_i^{\top}]$ exists and is non-singular with diagonalization $\mathbb{E}_{p_*}[x_ix_i^{\top}] = U_*^{\top}\operatorname{diag}(\lambda)U_* + \bar{U}_*^{\top}\operatorname{diag}(\bar{\lambda})\bar{U}_*$ such that $\min(\lambda) > \max(\bar{\lambda})$. Additionally, for a strictly concave (in its second argument), twice differentiable log-likelihood function ϕ with bounded second derivatives (in both arguments) and some $\beta \in \mathbb{R}^D$, let $y_i|x_i \sim \exp\{\phi(y_i, x_i^T\beta)\}$. Also, suppose that $\mathbb{E}\|y_i\|_2^2 < \infty$. Then if $p(\beta)$ is log-concave and positive on \mathbb{R}^D , the asymptotic error (in N) of the exact relative to approximate maximum a posteriori parameters, $\hat{\mu} = \lim_{N \to \infty} \hat{\mu}_N$ and $\bar{\mu} = \lim_{N \to \infty} \bar{\mu}_N$ is finite (where $\hat{\mu}_N$ and $\bar{\mu}_N$ are the approximate and exact MAP estimates, respectively, after N data-points), i.e., $\lim_{n \to \infty} \|\hat{\mu}_N - \bar{\mu}_N\|$ exists and is finite.

Proof. Before beginning, let \mathbb{P} denote a Borel probability measure on the sample space on which our random variables, $\{x_i\}$ and $\{y_i\}$, are defined such that these random variables are distributed as assumed according to \mathbb{P} . In what follows we demonstrate the asymptotic error is finite \mathbb{P} -almost surely. To this end, it suffices to show that $\hat{\mu}_N \overset{a.s.}{\to} \hat{\mu}$ and $\bar{\mu}_N \overset{a.s.}{\to} \bar{\mu}$ for some $\hat{\mu}$, $\bar{\mu}$ in \mathbb{R}^D .

Strong convergence of the exact MAP $(\bar{\mu}_N \stackrel{a.s.}{\rightarrow} \bar{\mu})$

This follows from Doob's consistency theorem (Van der Vaart, 2000, Theorem 10.10). The only nuance required in the application of this theorem here is that we must accommodate the regression setting. However by constructing a single measure \mathbb{P} governing both the covariates and responses, this simply becomes a special case of the usual theorem for unconditional models.

Strong convergence of the approximate MAP $(\hat{\mu}_N \stackrel{a.s.}{\rightarrow} \hat{\mu})$

In contrast to the strong consistency of $\bar{\mu}_N$, showing convergence of $\hat{\mu}_N$ requires more work. This is because we cannot rely on standard results such as Bernstein–Von Mises or Doob's consistency theorem, which require correct model specification. Since we have introduced the likelihood approximation $\tilde{p}(y|x,\beta) \neq p(y|x,\beta)$, the vector $\hat{\mu}_N$ is the MAP estimate under a misspecified model.

We demonstrate almost sure convergence in two steps; first we show that $U_*^{\top}\hat{\mu}_N$ converges almost surely to some $\gamma^* \in \mathbb{R}^M$; then we show that $\hat{\mu}_N = U_*U_*^{\top}\hat{\mu}_N + \bar{U}_N\bar{U}_N^{\top}\hat{\mu}_N$ must converge as a result. Since $U_NU_N^{\top} \stackrel{a.s.}{\to} U_*U_*^{\top}$ (as follows from entry-wise almost sure convergence of $\frac{1}{N}X^{\top}X \to \mathbb{E}_{p_*}[x_ix_i^{\top}]$ and the Davis–Kahan Theorem (Davis & Kahan, 1970)), this guarantees strong convergence of $\hat{\mu}_N = U_NU_N^{\top}\hat{\mu}_N + \bar{U}_N\bar{U}_N^{\top}\hat{\mu}_N$.

Part I: strong convergence of the projected approximate MAP, $U_*\hat{\mu}_N \overset{a.s.}{\to} \gamma^*$

Let $U_* \in \mathbb{R}^{D,M}$ be the top M eigenvectors of $\mathbb{E}_{p_*}[x_ix_i^{\top}]$, and recall that by assumption for any $y, \phi(y, x_i^T\beta)$ is a strictly concave function of $x_i^{\top}\beta$, in the sense that for any y and any b,b' in \mathbb{R} and t in (0,1) with $b \neq b', \phi(y,tb+(1-t)b') > t\phi(y,b)+(1-t)\phi(y,b')$. Then by Lemma F.2 we have that there is a unique maximizer $\gamma^* = \arg\max_{\gamma \in R^M} \mathbb{E}[\phi(y,x^{\top}U_*\gamma)]$

We next note that the Hessian of the expected approximate negative log likelihood with respect to γ is positive definite everywhere,

$$\nabla_{\gamma}^2 - \mathbb{E}_{y \sim p(y|x,\beta),x \sim p_*}[\phi(y,x^\top U_*\gamma)] = -\mathbb{E}[\left(\nabla_{\gamma}\phi'(y,x^\top U_*\gamma)\right)x^\top U_*] = -U_*^\top \mathbb{E}[x\phi''(y,x^\top U_*\gamma)x^\top]U_* \succ 0$$

since the strict log concavity and twice differentiability of ϕ ensure that $-\mathbb{E}[x\phi''(y,x^\top U_*\gamma)x^\top] \succ 0$.

Now consider any compact neighborhood $K \subset \mathbb{R}^M$ containing γ^* as an interior point. Then, by Lemma F.3 the set $\mathcal{F} = \{f_\gamma: X \times Y \to \mathbb{R}, (x,y) \mapsto \phi(y,x^\top U_*\gamma) | \gamma \in K\}$ is \mathbb{P} -Glivenko–Cantelli. As such $\sup_{f_\gamma \in \mathcal{F}} |\frac{1}{N} \sum_{i=1}^N f_\gamma(x_i,y_i) - \mathbb{E}[f_\gamma(x_i,y_i)]| \stackrel{a.s.}{\longrightarrow} 0$, that is to say, the empirical average log-likelihood converges uniformly to its expectation across all $\gamma \in K$. As a result, we have that for $\gamma_N := \arg\max_{\gamma \in K} \log \tilde{p}(U_*\beta = \gamma | X, Y) = \arg\max_{\gamma \in K} \frac{1}{N} \left[\log p(U_*^T\beta = \gamma) + \sum_{i=1}^N \phi(y_i, x_i^\top U_*\gamma)\right], \gamma_N \stackrel{a.s.}{\longrightarrow} \gamma^*.$

It remains in this part only to show that convergence of the approximate MAP parameter within this subset K implies convergence of $U_*^{\top}\hat{\mu}$, the approximate MAP parameter (across all of \mathbb{R}^M). However, this follows immediately from the strict log concavity of the posterior; because $\gamma^* \in K^\circ$, for N large enough each $\gamma_N \in K^\circ$ and we may construct a sub-level set such that $\gamma_N \in C_N \subset K$ such that $\forall \gamma \notin C_N, \log p(U_*^{\top}\beta = \gamma) + \sum_{i=1}^N \phi(y_i, x_i^{\top}U_*\gamma) < \log p(U_*^{\top}\beta = \gamma_N) + \sum_{i=1}^N \phi(y_i, x_i^{\top}U_*\gamma_N)$.

Part II: convergence of $\bar{U}_*\bar{U}_*^{\top}\hat{\mu}_N + U_*\gamma$

Using the result of Part I, we can write that $\hat{\mu}_N = U_*U_*^\top\hat{\mu}_N + \bar{U}_*\bar{U}_*^\top\hat{\mu}_N \to U_*\gamma^* + \bar{U}_*\bar{U}_*^\top\hat{\mu}_N$. However, since $\bar{U}_*\bar{U}_*^\top\beta \perp X, Y|U_*^\top\beta$ under \mathbb{P} , convergence of $U_*^\top\hat{\mu}_N \to \gamma^*$ implies convergence of $\arg\max_{\bar{U}_*^\top\beta}\tilde{p}(\bar{U}_*^\top\beta|U_*^\top\beta = U_*^\top)$ to some $\bar{U}_*^\top\hat{\mu}_N$ since continuity of $p(\beta)$ and $\tilde{p}(Y|X,\beta)$ imply continuity of the arg-max. Thus both $\hat{\mu}_N$ and $\bar{\mu}_N$ converge, guaranteeing convergence of the asymptotic error. \square

Lemma F.2. For any $\phi(\cdot,\cdot)$ which is strictly concave in its second argument, if there is a global maximizer $\beta^* = \arg\max_{\beta \in \mathbb{R}^D} V(\beta) = \mathbb{E}_{x \sim p_*, y \sim p(y|x,\beta)}[\phi(y, x^\top \beta)]$, then there is a unique global maximizer,

$$\gamma^* = \arg\max_{\gamma \in \mathbb{R}^M} V(U_*\gamma)$$

Proof. We first note that $V(\cdot)$ must have bounded sub-level sets. Thus $W(\cdot) := V(U_* \cdot)$ must also have bounded sub-level sets since $V^{-1}([a,\infty]) = \{\beta | V(\beta) \geq a\} \supset \{\beta | \exists \gamma \in \mathbb{R}^M \text{ s.t. } \beta = U_* \gamma \text{ and } V(U_* \gamma) \geq a\} = U_* W^{-1}([a,\infty])$. Thus, since W is strictly concave and has bounded sub-level sets, it has a unique maximizer.

Lemma F.3. Let $K \subset \mathbb{R}^M$ be compact and denote by X and Y the domains of the covariates and responses, respectively. Then under the assumptions of Theorem F.2, the set $\mathcal{F} = \{f_\gamma : X \times Y \to \mathbb{R}, (x,y) \mapsto \phi(y,x^\top U\gamma) | \gamma \in K \}$ is \mathbb{P} -Glivenko–Cantelli.

Proof. This result follows from Theorem 19.4 in (Van der Vaart, 2000), and builds from example 19.7 of the same reference; in particular, the condition of bounded second derivatives of ϕ implies that for any f_{γ} , $f_{\gamma'}$ in \mathcal{F} and x in X, y in Y, we have $|f_{\gamma}(x,y)-f_{\gamma'}(x,y)| \leq C||x||_2^2$. The previous condition is sufficient to ensure finite bracketing numbers, and the result follows. Notably, in keeping with example 19.7 we have that for all x, y and for all γ and γ' in K,

$$|f_{\gamma}(x,y) - f_{\gamma'}(x,y)| = |\int_{x^{\top}U\gamma'}^{x^{\top}U\gamma} \phi'(y,a)da|$$

$$= |\int_{x^{\top}U\gamma'}^{x^{\top}U\gamma} \phi'(y,x^{\top}U\gamma') + \int_{x^{\top}U\gamma'}^{a} \phi''(y,b)db da|$$

$$\leq ||x^{\top}U(\gamma - \gamma')\phi'(y,x^{\top}U\gamma')||_{2} + \frac{1}{2}||x^{\top}U(\gamma - \gamma')||_{2}^{2} \sup_{a \in \mathbb{R}} \phi''(y,a)$$

$$\leq ||x^{\top}U||_{2}(||y||_{2} + ||x^{\top}U||_{2}||\gamma'||_{2})\phi''_{\max}||\gamma - \gamma'||_{2} + \frac{1}{2}||x^{\top}U||_{2}^{2}||\gamma - \gamma'||_{2}^{2}\phi''_{\max}$$

$$\leq \left[\frac{3}{2}||x^{\top}U||_{2}^{2}\operatorname{diam}(K)\phi''_{\max} + ||x^{\top}U||_{2}||y||_{2}\phi''_{\max}\right]||\gamma - \gamma'||_{2}$$

$$\leq C(||x^{\top}U||_{2}^{2} + ||x^{\top}U||_{2}||y||_{2})||\gamma - \gamma'||_{2},$$
(F.7)

where in the first and second lines we use the fundamental theorem of calculus, and in the fourth and fifth lines we rely on the boundedness of the second derivatives of ϕ and that the compactness subsets of \mathbb{R}^M implies boundedness. In the final line C is an absolute constant.

Finally, we note that $\mathbb{E}_{\mathbb{P}}\|x^{\top}U\|_2^2 < \infty$ since $\mathbb{E}_{\mathbb{P}}\|x^{\top}U\|_2^2 = \mathbb{E}_{\mathbb{P}}x^{\top}UU^{\top}x < \mathbb{E}_{\mathbb{P}}x^{\top}x = \operatorname{Tr}(\mathbb{E}_{p_*}xx^{\top}) < \infty$, and by Cauchy Schwartz, $\mathbb{E}_{\mathbb{P}}\|x^{\top}U\|_2\|y\|_2 \leq \sqrt{\mathbb{E}_{\mathbb{P}}\|x^{\top}U\|_2^2\mathbb{E}_{\mathbb{P}}\|y\|_2^2} \leq \infty$. This confirms (as in example 19.7 (Van der Vaart, 2000)) that for all $\epsilon > 0$, the ϵ -bracketing number of \mathcal{F} is finite. By Theorem 19.4 of (Van der Vaart, 2000), this proves that \mathcal{F} is \mathbb{P} -Glivenko-Cantelli.

F.8. Factorized Laplace approximations underestimate marginal variances

We here illustrate that the factorized Laplace approximation underestimates marginal variances. Consider for simplicity the case of a bivariate Gaussian with

$$\Sigma = \begin{bmatrix} a & b \\ b & c \end{bmatrix},$$

for which the Hessian evaluated anywhere is

$$\Sigma^{-1} = \frac{1}{ac - b^2} \begin{bmatrix} c & -b \\ -b & a \end{bmatrix}.$$

Ignoring off diagonal terms and inverting to approximate Σ_N , as is done by a diagonal Laplace approximation, yields:

$$\tilde{\Sigma} = \begin{bmatrix} a - \frac{b^2}{c} & 0\\ 0 & c - \frac{b^2}{a} \end{bmatrix}.$$

This approximation reports marginal variances which are lower than the exact marginal variances.

That this approximation underestimates marginal variances in the more general D>2 dimensional case may be easily seen from considering the block matrix inversion of Σ , with blocks of dimension 1×1 , $(D-1)\times 1$, $1\times (D-1)$ and $(D-1)\times (D-1)$, and noting that the Schur complement of a positive definite covariance matrix will always be positive definite.

G. LR-MCMC

We provide the LR-MCMC algorithm for performing fast MCMC in generalized linear models with low-rank data approximations.

Algorithm 2 LR-MCMC for Bayesian inference in GLMs with low-rank data approximations.

1: Input: prior $p(\beta)$, data $X \in \mathbb{R}^{N,D}$, rank $M \ll D$, GLM mapping ϕ , MCMC transition kernel $q(\cdot,\cdot)$, number of MCMC iterations T. Time and memory complexities that are not included depend on the specific choice of MCMC transition kernel.

2: Pseudo-Code	3: Time Complexity	4: Memory Complexity
5: Data preprocessing — M-Truncated SVD		
6: $U, \operatorname{diag}(\lambda), V := \operatorname{truncated-SVD}(X^{\top}, M)$	O(NDM)	O(NM + DM)
7: $X_U = XU$	O(NM)	O(NDM)
8: Propose $\beta^{(t)} \in \mathbb{R}^D$, compute likelihood 9: $\beta^{(t)} \sim q(\beta^{(t)}, \beta^{(t-1)})$	_	_
9: $\beta^{(t)} \sim q(\beta^{(t)}, \beta^{(t-1)})$ 10: $\mathcal{L}_t := \sum_{i=1}^N \phi(y_i, x_i^\top U U^\top \beta^{(t)}) + \log p(\beta^{(t)})$	O(1)	O(NM + MD)
11: Accept or Reject		
12: Acceptance probability $p_A := \min\left(1, \frac{\mathcal{L}_t}{\mathcal{L}_{t-1}}\right)$	O(1)	O(1)
13: Accept $\beta^{(t)}$ with probability p_A	O(1)	O(1)
14: Repeat steps 3-6 for T iterations		

The transition in Line 9 may additionally benefit from the LR-GLM approximation. In particular, widely used algorithms such as Hamiltonian Monte Carlo and the No-U-Turn Sampler rely on many O(ND)-time likelihood and gradient evaluations, the cost of which can be reduced to O(NM+DM) with LR-GLM. An implementation of this approximation is given in the Stan model in Appendix A.3 with performance results in Figures A.3 and A.6.

H. LR-Laplace with non-Gaussian priors

As discussed in the main text, we can maintain computational advantages of LR-GLM even when we have non-Gaussian priors. This admits the procedure provided in Algorithm 3.

In order for this more general LR-Laplace algorithm to be computationally efficient, we still require that the prior have some properties which can accommodate efficiency. In particular Line 11 demands that the Hessian of the prior is computed and inverted, as will true even in the high-dimensional setting when, for example, the prior factorizes across dimensions. Additionally, properties of the prior such as log concavity will facilitate efficient optimisation in Line 8.

 $^{^7 \}text{To keep notation concise we use } \vec{\phi}_{\hat{\mu}}^{\prime\prime} \text{ to denote } \vec{\phi}^{\prime\prime}(Y,XUU^\top \hat{\mu})$

Algorithm 3 LR-Laplace for Bayesian inference in GLMs with low-rank data approximations and twice differentiable prior. Time and memory complexities which are not included depend on the choice of prior and optimisation method, which can be problem specific.

oe j	problem specific.		
1:	Input: twice differentiable prior $p(\beta)$, data $X \in \mathbb{R}^{N,D}$, real and Section 5.1)	ank $M \ll D$, GLM map	ping ϕ with ϕ'' (see Eq. (5)
2:	Pseudo-Code	3: Time Complexity	4: Memory Complexity
	$\begin{aligned} \textit{Data preprocessing} &- \textit{M-Truncated SVD} \\ \textit{U}, \operatorname{diag}(\lambda), \textit{V} &:= \operatorname{truncated-SVD}(\textit{X}^T, \textit{M}) \end{aligned}$	O(NDM)	O(NM+DM)
	Optimize to find approximate MAP estimate (in D-dimensional $\hat{\mu} := \arg\max_{\mu \in \mathbb{R}^D} \sum_{i=1}^N \phi(y_i, x_i U U^\top \mu) + \log p(\beta = \mu)$	d space) —	_
10: 11:	Compute approximate posterior covariance ⁷ $\hat{\Sigma}^{-1} := -\nabla_{\beta}^{2} \log p_{\beta}(\hat{\mu}) - UU^{\top}X^{\top} \operatorname{diag}(\vec{\phi}_{\hat{\mu}}'')XUU^{\top} \\ K := [\nabla_{\beta}^{2} \log p(\beta) _{\beta = \hat{\mu}}]^{-1} \\ \hat{\Sigma} := -K + KU([U^{\top}X^{\top}\operatorname{diag}(\vec{\phi}_{\hat{\mu}}'')XU]^{-1} + U^{\top}KU)^{-1}U^{\top}KU)^{-1}U^{\top}KU$	_ _ _	_ _ _
13: 14:	Compute variances and covariances of parameters $\operatorname{Var}_{\hat{p}}(\beta_i) = e_i^{\top} \hat{\Sigma} e_i$	_	_
15:	$\operatorname{Cov}_{\hat{p}}(\beta_i, \beta_j) = e_i^{T} \hat{\Sigma} e_j$		